Assessment of Constellation Designs for Earth Observation: Application to the TROPICS Mission

Pau Garcia Buzzi[a], Daniel Selva[a], Nozomi Hitomi[b], William J. Blackwell[c]

[a]*Department of Aerospace Engineering, Texas A&M University*
[b]*Sibley School of Mechanical and Aerospace Engineering, Cornell University*
[c]*Lincoln Laboratory, Massachusetts Institute of Technology*

Abstract

The orbit and constellation design process for Earth observation missions is complex and it involves trades between mission lifetime, instrument performance, coverage, cost, and robustness among others. This paper describes an orbit and constellation design study conducted during Pre-Phase A and Phase A for the NASA-funded Time-Resolved Observations of Precipitation structure and storm Intensity with a Constellation of SmallSats (TROPICS) mission. Thousands of potential constellations were enumerated, simulated using an open-source astrodynamics library, and compared with one another across multiple dimensions, focusing on cost and coverage considerations. The robustness of different constellations to various hypothetical operational failures (e.g., loss of one satellite or one launch) was systematically assessed. A deployment strategy based on differential drag was proposed and analyzed for selected constellations. Finally, the orbital lifetime of various architectures was also studied with respect to NASA's 25-year de-orbiting recommendation. The contributions of this work include: (1) an exhaustive analysis of figures of merit commonly used in Earth observation orbit design; (2) A methodology to assess robustness of constellations based on a brute-force disjoint scenario simulation approach; (3) Results and recommendations from the mission analysis process for the TROPICS mission.

Keywords: TROPICS, small satellites, satellite constellation, coverage analysis, orbit selection, robustness

1. Introduction

The Time-Resolved Observations of Precipitation structure and storm Intensity with a Constellation of SmallSats (TROPICS) mission is a NASA Earth Venture Instrument mission that aims to monitor the thermodynamics of the troposphere and the precipitation structure for storm systems over the tropical regions. To do so, TROPICS uses a fleet of several LEO dual spinning 3U-CubeSats, each hosting a payload consisting of a 12-channel high-performance millimeter-wave radiometer that provides different measurements such as temperature and water vapor profiles, imagery for precipitation quantification, and cloud ice measurements [1].

The orbit and constellation design process for Earth observation missions is complex and it involves trades between mission lifetime, instrument performance, coverage, cost, and risk among others. One of the most important trades is arguably the one between the energy (and thus cost) required to put a constellation of small satellites into the desired orbits and the Earth coverage performance obtained from the resulting constellation. Generally, numerical simulation software, such as AGI's Systems Toolkit (STK), GMAT, or Orekit, is used to compute coverage metrics in complex scenarios involving multiple satellites and including highly accurate Earth and satellite propagation models. This software calculates the access time intervals for each satellite in the constellation and each point of interest in the user-defined coverage grid on the surface of Earth, taking into account various constraints related to viewing geometry and imaging concept. These access intervals are the basis for calculating most coverage metrics or Figures Of Merit (FOM)– both terms are used interchangeably in this paper. Often, several FOM such as mean and maximum revisit time are calculated for a coverage grid containing thousands of points on the surface of the Earth. For instance, to get a global grid with 100km spacing between adjacent points, around 48000 points are needed. This may lead to information overload, as it is not trivial how to aggregate all that information into a single number representative of the constellation's coverage performance. Indeed, several metrics are used, including mean and max revisit time, or mean response time, among many others.

Such coverage metrics need to be traded against cost and risk during Pre-Phase A and Phase A studies to determine the number of satellites and orbital characteristics. In addition, there are other important considerations that must be taken into account in that decision, including the deployment strategy for the constellation, the robustness of the constellation to satellite and launch failures, as well as mission lifetime and deorbiting.

It is worthwhile to note that, in the experience of the authors, attempting to formulate a multi-attribute decision making problem a priori is challenging because it is hard, if not impossible, to know a priori the preferences between all these attributes. For example, ideally, we would like to run an Observing Sys-

Email addresses: pg428@tamu.edu (Pau Garcia Buzzi), dselva@tamu.edu (Daniel Selva), nh295@cornell.edu (Nozomi Hitomi), wjb@ll.mit.edu (William J. Blackwell)

tem Simulation Experiment for each configuration to see how different values of spatial resolution, temporal resolution, and accuracy combine to improve weather forecasting accuracy or a similar high-level parameter –but that is of course not possible. It is thus desirable to adopt a more human-driven process, akin to tradespace exploration or design by shopping, in which the main trades and alternatives are discovered at the same time as decision maker preferences are elicited.

With this in mind, this paper describes a constellation design study performed during Pre-Phase A and Phase A of the TROPICS mission. The goal of the study was to recommend the best candidate architectures considering two major requirements of the TROPICS mission: having a mean revisit time equal or less than 60 minutes over the tropical regions, and distributing the satellites of the constellation in 3 or fewer planes (due to a constraint on the number of launches combined with the absence of a propulsion system).

In addition to the mission-specific recommendation, the paper provides general orbit and constellation design guidelines that could be applied to any future Earth observing mission. This work includes a survey and discussion of the most common metrics used in constellation design of Earth Observation Missions, such as coverage performance metrics, cost, constellation deployment, robustness and lifetime. Furthermore, the paper describes a new way to assess constellation robustness through the quantification of the degradation of coverage metrics associated with changes to an original/reference constellation configuration based on a brute-force disjoint scenario simulation approach. Likewise, the time needed to deploy the TROPICS Cubesats within a plane is calculated using a differential drag-based strategy exploiting changes in solar panel configuration in eclipse and sunlight periods. Finally, orbital lifetime changes are computed for various altitudes and drag area configurations.

A contribution of this paper to the literature is a critical analysis of the different FOM commonly used in constellation design and the evaluation of how changes in orbital design parameters such as inclination, altitude, and number of satellites and planes affect these coverage metrics. To the best of our knowledge, this is the first comprehensive effort to characterize the characteristics and shortcomings of the most commonly used coverage metrics, such as revisit or gap time statistics. Most papers in the field only look at optimizing orbital parameters to maximize coverage [2, 3, 4, 5, 6, 7, 8, 9, 10, 11], whereas this paper also incorporates other important aspects in the orbit selection process, such as robustness and deployment strategies. An exception is found in [12], where coverage performance, cost and risk metrics were considered to solve a multi-objective constellation reconfiguration design problem. However, that problem concerned GPS constellations as opposed to Earth observation, and studied optimal reconfiguration of constellations as opposed to optimizing the (initial) constellation design.

The remainder of this paper is structured as follows: Section 2 contains a review of the most relevant FOMs for constellation design and orbit selection in Earth observation missions, including cost and coverage, but also robustness and lifetime considerations. Section 3 lists some important guidelines to take into account when setting up a numerical coverage simulation. Section 4 presents the TROPICS mission constellation design study, including: a coverage analysis, the degradation of performance due to hypothetical satellite losses in the constellation or launch vehicle failures, the feasibility study of a differential drag based deployment strategy, and a mission lifetime assessment. Finally, section 5 concludes the paper with a discussion of the limitations of the study, and opportunities for future work.

2. Figures of Merit for Early Design of Earth Observation Constellations

This section describes the main FOMs used in the early development stages (Pre-Phase A and Phase A) of Earth observation constellations. Subsections 2.1, 2.2, 2.3, 2.4 and 2.5 discuss coverage performance metrics, cost, constellation robustness, lifetime and deployment, respectively.

2.1. Coverage

2.1.1. Coverage metrics for a single point of the grid

Coverage metrics quantify how well the constellation "covers" the surface of the Earth with its observations. Coverage metrics are usually calculated on a grid of points on the surface of the Earth, by propagating the different spacecraft that compose the constellation for a certain simulation time T. During the propagation, the access time intervals in which coverage grid points are seen by any of the satellites are computed, when considering the field of view and imaging concept of the sensors, and any viewing geometry constraints, such as those on incidence angle. When ordering this list of time intervals, $(ts_{ki,n}, te_{ki,n})$ indicates the start and end time respectively for the nth access of satellite i to coverage grid point k. Often, the satellite(s) that perform(s) the access are irrelevant for the calculations, and thus the subindex i can be ignored. For every point on the grid k, a coverage gap is the interval of time between the end of an access n between the point k and any satellite in the constellation, and the start of the next access $n+1$: $tg_{k,n} = ts_{k,n+1} - te_{k,n}$. All coverage metrics are calculated from statistics of the access and gap intervals. These statistics are calculated for each point in the coverage grid, but can be aggregated (e.g., averaged out) for all points at a given latitude (e.g., to obtain a chart of average revisit time vs latitude), or for all points in the coverage definition (to obtain, for example, a single average revisit time number for the constellation). Of note, other names for access and gap intervals found in the literature are *dwell time* and *unattendance time* respectively [13].

Because there are many different ways to aggregate information from points in the coverage grid, and many statistics that can be calculated, many different coverage metrics have been defined. Moreover, it is unclear a priori which metrics are best for a given mission. The following are some of the most widely used metrics in the literature [14, 2, 5] – all of them are defined for a single point k on the grid:

- **Descriptive statistics**. Minimum, maximum, median, mean, variance and different percentiles of access and/or

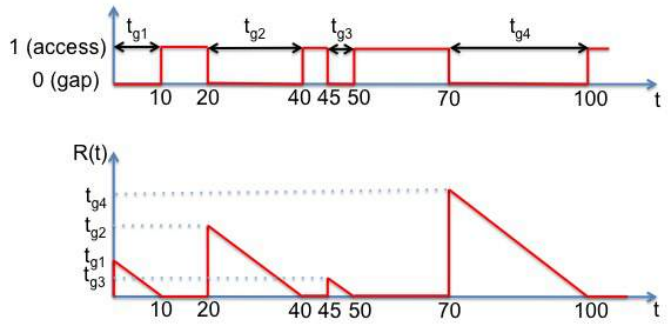

Figure 1: Top: Notional example of gap and access intervals for a particular point on the Earth grid. Bottom: The correspondent response time $R_k(t)$.

gap interval duration for point k. The most important ones are: (1) mean coverage gap, also known as mean revisit time, which is the average length of the gap intervals for point k, and the most common metric used in coverage analysis by far; and (2) maximum revisit time, also known as maximum gap time, which corresponds to the longest gap interval for point k, and is also popular as it provides worst-case information.

- **Percent Coverage** (PC). Total time during which point k is accessed by at least one satellite in the constellation divided by the total simulation time:

$$PC_k = 1 - \frac{\sum_n tg_{k,n}}{T} \tag{1}$$

where T is the simulation time and $tg_{k,n}$ is the nth gap time for point k in the coverage grid, as defined above.

- **Mean Response Time**. Response time is defined as the time from when a random request is received to observe a point k until the constellation can actually observe it. Note that response time is a function of time. If at a given time t, the point k is being accessed by the constellation, i.e., $ts_{k,n} \leq t \leq te_{k,n}$ for some n, then the response time at that time is zero ($R_k(t) = 0$). If the point k is in a coverage gap at time t, i.e., $te_{k,n} \leq t \leq ts_{k,n+1}$ for some n, then the response time is the time until the end of that gap, i.e., until the point is accessed again: $R_k(t) = ts_{k,n+1} - t$. Thus, mean response time is defined as the time average of the response time.

$$R_k = \frac{1}{T}\int R_k(t)dt = \frac{\sum_n tg_{k,n}^2}{2T} \tag{2}$$

The $\frac{tg_{k,n}^2}{2}$ quadratic term comes from the integration of a linear function (the time to next contact). In other words, it corresponds to the area of the different triangles defining the response time curve (see Figure 1).

- **Time Average Gap**. For a given point of the grid k, it corresponds to the time average of the mean gap duration, which is also a function of time. This FOM is very similar to mean response time because the function being averaged (integrated) is the length of the current gap at every time instant $G_k(t)$, which is 0 in the case of the point being accessed at time t and equal to $tg_{k,n}$ otherwise. Time average gap can be obtained by multiplying the mean response time by a factor of 2, since the area under the curve we are integrating now corresponds to sum of the area of the rectangles whose area is twice the one of the triangles on the mean response time calculation.

$$G_k = \frac{1}{T}\int G_k(t)dt = \frac{\sum_n tg_{k,n}^2}{T} \tag{3}$$

One issue with some of the above metrics is that they can be biased or misleading for gap duration distributions with many short gaps and a few very long gaps – typical of string-of-pearls constellations, which are popular constellation designs for CubeSats, since they are advantageous in terms of launch cost. In most applications, many successive short gaps during coverage periods do not compensate for a few very long gaps between coverage periods. Thus, using a simple mean or median of all gap durations as a FOM in these cases may lead to overly optimistic results, especially when the number of satellite grows. In Figure 2, two Cumulative Distribution Functions (CDF) of the revisit times for 2 very different constellations are shown. In constellation 1, 6 satellites are put into the same orbital plane, whereas in constellation 2, these 6 satellites are distributed in 6 different planes equally spaced in Right Ascension of the Ascending Node (RAAN). We can observe that only looking at mean revisit times, both constellations would appear to be very similar. However, for constellation 1, 90% of gaps are less or equal to 16 mins, and the only few very long gaps of nearly 1000 mins bias their mean statistics towards the ones corresponding to constellation 2, which has fewer very short gaps but they are all shorter than 156 minutes.

For this reason, another metric considered in the TROPICS coverage study that has not been described in the literature is what the team called Continuous High Revisit Coverage (CHRC), which was defined as the percentage of time where point k is either in an access, or in a gap shorter than a threshold gap duration t_{hold}.

$$CHRC_k = 1 - \frac{\sum_n (tg_{k,n} \geq t_{hold})}{T} \tag{4}$$

For some applications, gaps shorter than some threshold may not be important. For instance, if the satellite data is to be assimilated in a weather model that has a time step of 1 hour, gaps shorter than 1 hour may not affect the output of the model, so one could argue that they should be ignored. This new metric ignores short gaps and thus can better account for the importance of those long gaps left, for example, by string-of-pearls constellations.

Other coverage metrics found in the literature are total time of coverage over a *region*, and access to daytime and nighttime coverage [15]. Total time of coverage over a *region* gives the same information as the percent coverage but for a region (a set of points) instead of a single point. Usually, if any point in

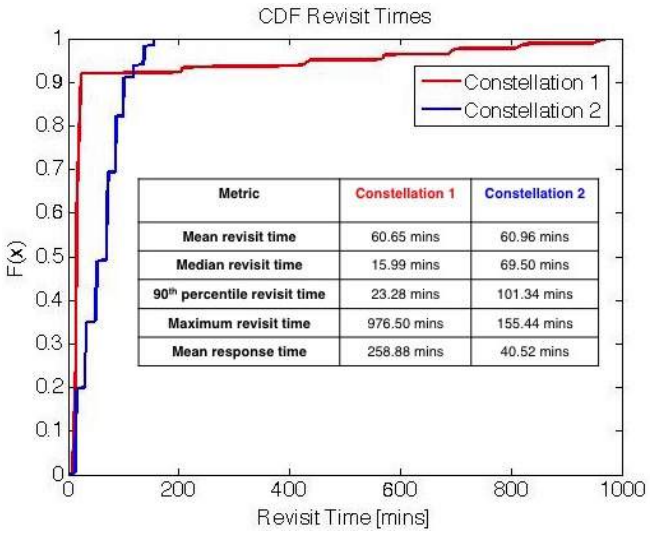

Metric	Constellation 1	Constellation 2
Mean revisit time	60.65 mins	60.96 mins
Median revisit time	15.99 mins	69.50 mins
90th percentile revisit time	23.28 mins	101.34 mins
Maximum revisit time	976.50 mins	155.44 mins
Mean response time	258.88 mins	40.52 mins

Figure 2: Comparison of the coverage metrics for 2 constellations. Constellation 1 (6 satellites distributed in 1 plane) has a lot of very short gaps and only a few very long gaps. Constellation 2 (6 satellites distributed in 6 planes) has fewer very short gaps and their duration is more balanced with no very long gaps.

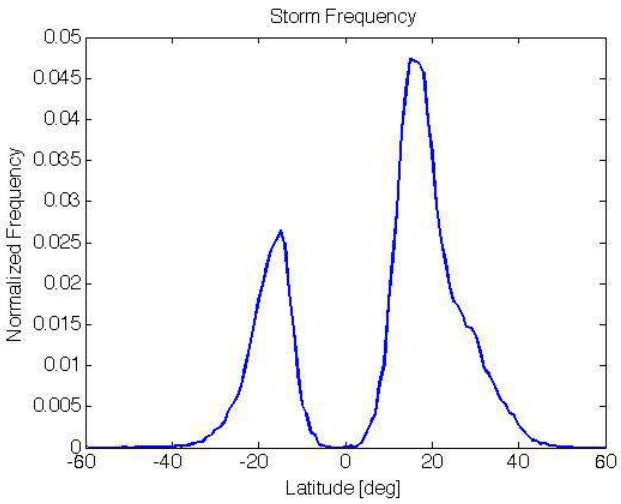

Figure 3: Storm frequency vs latitude. These values were used as latitude weights to compute latitude-weighted coverage metrics.

the region is observed, the region is considered observed. Fraction of time in daylight/eclipse and the time needed to see an entire diurnal cycle are also relevant metrics often considered. Zhang et al. [16] define Coverage Rate of sampling points as the ratio between the number of time steps where the point was in access and the total number of time steps. Note that this metric is essentially identical, although potentially less precise, than percent coverage as defined above. The coverage state is only checked at constant time steps, and thus the exact start and end times within the time steps of the different accesses are ignored. The smaller the time step, the closer coverage rate will be to percent coverage.

Of note, many other coverage metrics exist in the literature that are specific to intelligence, surveillance and reconnaissance tasks. Examples are analysis time, target leakage, target coverage frequency and target ghost time [13]. These metrics were left out of scope of this paper, which deals with observation of the Earth system's geophysical parameters, as opposed to dynamic targets.

2.1.2. *Aggregation of coverage metrics for a set of points on the grid*

So far, several relevant access/gap metrics have been described for a given point on the grid. For many purposes, such as using coverage metrics as objectives in optimization problems or when conducting a tradespace exploration of several constellation configurations, it is convenient to condense information for different points of the grid into a single quantity that summarizes the coverage of an architecture or constellation. For example, statistics of single-point metrics can be aggregated (e.g., averaged) across a region of interest, be it worldwide (Global), or regional (e.g., "tropical regions", "cold regions", or "continental US"). Another way of condensing information is to do a weighted average of the metric values for different points in the grid, for example weighting average revisit times by the cosine of the corresponding latitude (AWART) [2], which effectively makes tropical regions more important than cold regions. More generally, latitude-weighted metrics should reflect the importance of different latitudes to the mission objective at hand. For example, as the main objective of TROPICS is to monitor extreme weather events around the tropics, in this study latitudes were weighted proportionally to the storm frequency data shown in Figure 3. This latitude plot was generated by considering tropical storms with wind speeds exceeding 34 knots that occurred from 1985 through 2014.

2.1.3. *Coverage for narrow-swath instruments*

Narrow-swath instruments such as lidars and certain radars and high-resolution imagers often require special considerations when assessing coverage. Indeed, for these missions, it is often infeasible to achieve global coverage for all longitudes in a reasonable amount of time. Instead, such sensors are often put on repeat ground track orbits that guarantee a certain revisit time (equal to the repeat ground track period) for the regions covered, but leaves some regions uncovered. Thus, if we attempt to calculate the metrics defined in the previous subsection, we observe a strong dependency on the total simulation time, since the gap time for all non-visited points is equal by default to the total simulation time.

In these cases, the first metric that is important to capture is the total area or percentage of the earth's surface that is being covered. In general, for a single satellite, there is a trade-off between achieving good coverage (which requires a large repeat period) and achieving good revisit time within the area covered (which requires a small repeat period). Once this trade-off is understood, the metrics defined in the previous subsection can be used only on the regions visited by the sensor.

2.2. *Cost*

Naturally, coverage of a constellation is traded against number of satellites and ultimately cost. Cost can be considered as

an objective to be minimized, or as a constraint to satisfy (cost cap). Access to Earth orbit for small satellites, and specifically the cost and availability of launch services, is still arguably the most significant threat to the growth of concepts based on large constellations of small satellites [17].

However, cost is always challenging to estimate, especially during Pre-Phase A studies where there is a lot of uncertainty in design details. Hence, proxies are often used instead of cost in trade studies. Wertz [14] uses the mission ΔV budget to define the Orbit Cost Function (OCF), which estimates the relative cost of putting a spacecraft into a given orbit with respect to the cost of putting it into a 185 km circular low-Earth orbit. Specifically, the OCF is defined as the ratio of the mass delivered to a 185 km altitude circular orbit to the mass delivered to the mission orbit, for the same amount of propellant. It can be seen as a multiplier to obtain the cost of putting a spacecraft into its mission orbit from the cost of putting the spacecraft in LEO, which can be estimated using historical launch vehicle cost data.

The cost model used in this paper tries to capture the effect of the main design decisions such as the satellite's altitude, inclination, and the size and configuration of the constellation. The total cost of the mission is composed of constellation cost C_{Const} and launch cost C_{Launch} as shown in equation 5:

$$Cost = C_{Launch} + C_{Const} \tag{5}$$

As shown in equation 6, the constellation cost is computed by multiplying the cost of a single satellite by a learning curve factor L to account for productivity improvements as a larger number of units is produced as usually done in the literature (e.g., [18]). A learning curve slope S of 90% has been assumed in all cost calculations for the TROPICS case study shown in section 4. The cost of a single satellite is approximated by equation 7, a *Cost Estimation relationship (CER)* found in [14], useful to calculate the bus cost for spacecraft weighting less than 500kg. Even though the mass input range for this CER is from 20kg to 400kg, it was still used in this work to calculate the cost of spacecraft with less than 20kg mass, as more accurate cost models for CubeSats were not available. The lack of cost models for Distributed Space Missions (DSMs) has been an ongoing problem for the last decade due to the absence of reliable learning curve factors and CERs for small satellites of less than 20kg [19]. This model predicts a bus cost of \$1.3M for a 5kg satellite. This estimate is not unreasonable assuming payload cost is included and once integration and testing, systems engineering, and program overhead costs are added to the cost of purchasing the bus.

$$C_{Const} = C_{Sat} \cdot L = C_{Sat} \cdot n_{Sat}^{B} = C_{Sat} \cdot n_{Sat}^{1-log_2(\frac{100\%}{S})} \tag{6}$$

$$C_{Sat} = 1064 + 35.5 \cdot m_{sat}^{1.261} \tag{7}$$

The launch cost, on the other hand, is calculated by multiplying the cost of a single launch C_{LV} by the number of planes n_{Planes} in the constellation as seen in equation 8.

$$C_{Launch} = n_{Planes} \cdot C_{LV} \tag{8}$$

In doing so, the assumption of needing an extra launch vehicle for every additional plane in the architecture is made. This is a reasonable assumption since many small satellites do not have propulsion capabilities to do expensive out-of-plane orbit maneuvers such as changing the RAAN [20]. A possibility not considered in this paper is the ability of the upper stage of the launch vehicle to make plane changes and deliver satellites to multiple planes.

The proxy used in this study for launch cost is mostly driven by the cost of the propellant needed to put the spacecraft into the desired mission orbit. The reason behind making this approximation is the difficulty to obtain accurate pricing information for launch services, which also depends on purely commercial considerations. Our strategy, based on energy computations, makes this estimate independent of the pricing strategy while still being a reasonable proxy for launch cost.

The amount of propellant needed is computed in several steps. First, the ΔV required to go from the launch site to the desired altitude h and inclination i is computed as shown in equation 9.

$$\Delta V_{h,i} = \Delta V_{0-400km,28.7^\circ} + \Delta V_{400km,28.7^\circ-h,i} \tag{9}$$

where $\Delta V_{0-400km,28.7^\circ}$ is the ΔV required to go from altitude 0km to a LEO of 400km and 28.7° inclination –which is representative of a low ΔV launch from Cape Canaveral, and in this paper is assumed to be a known constant of 10,000 m/s. $\Delta V_{400km,28.7^\circ-h,i}$ is the ΔV required to go from 400km to the desired altitude $h > 400km$ and inclination $i > 28.7^\circ$. This second term is computed by performing a Hohmann transfer [21] to increase the semi-major axis of the orbit and combining a simple plane change with the tangential burn at apogee of the transfer orbit, which corresponds to the most efficient way of changing orbit size and inclination simultaneously. $\Delta V_{400km,28.7^\circ-h,i}$ is computed using the following equations:

$$\Delta V_{400km,28.7^\circ-h,i} = \Delta V_1 + \Delta V_2 \tag{10}$$

$$\Delta V_1 = \sqrt{\mu}\left(\sqrt{\frac{2}{a_L} - \frac{1}{a_T}} - \sqrt{\frac{1}{a_L}}\right) \tag{11}$$

$$\Delta V_2 = \left\{\mu\left(\frac{2}{a_H} - \frac{1}{a_T}\right) + \frac{\mu}{a_H} - 2 \cdot \sqrt{\mu\left(\frac{2}{a_H} - \frac{1}{a_T}\right)} \cdot \sqrt{\frac{\mu}{a_H}} \cdot cos(i - 28.7)\right\}^{1/2} \tag{12}$$

where a_L and a_H are the semi-major axes of the initial 400 km and final h km orbits, a_T is the average of the initial and final semi-major axes and μ is the Earth gravitational parameter.

In our cost model, we considered both dedicated launch and ridesharing/piggybacking options, often used for CubeSats [22]. Dedicated launches provide more freedom to the customer to select the destination orbit and the launch date but are more costly than ridesharing/piggybacking options, which provide less (or no) flexibility in choosing orbits and mission

schedule. For instance, the rideshare option availability highly depends on the destination orbit; while there are more opportunities to launch SmallSats as secondary payloads to the International Space Station (ISS) orbit, Sun-synchronous orbit (SSO) or Geostationary transfer orbit (GTO), it is very difficult to find these launch services for other inclinations such as 30°. The launch vehicle cost is thus given by:

$$C_{LV} = \min(Cost_{dedicated}, Cost_{rideshare}) \tag{13}$$

To compute the dedicated and rideshare launch costs, the Electron launch vehicle from Rocket Lab was used as a benchmark [23] for launch services specializing in small satellites. In the model, the rideshare alternative is used if the payload mass ($m_{pload} = (n_{Sat}/n_{Planes}) \cdot m_{sat}$) is less than a small fraction (α) of the maximum payload mass ($m_{ploadmax}$) supported by the launch vehicle, a value that changes depending on the final orbit altitude and which was found in the Rocket Lab's user guide. Therefore, a baseline payload m_{pload0} of $(1 - \alpha) \cdot m_{ploadmax}$ is assumed, on top of which the rideshare payload is added.

Using the rocket equation, $\Delta V_{h,i}$ is translated into kg of propellant required for the launch. For the dedicated launch option, the mass of propellant is computed the following way:

$$m_{propD} = (m_s + m_{pload})(e^{\left(\frac{\Delta V_{h,i}}{g_0 I_{sp}}\right)} - 1) \tag{14}$$

where m_s is the predefined structure mass of the launch vehicle, 1200 kg, m_{pload} is the mass of the payload, $g_0 = 9.81 m/s^2$ and I_{sp} is the specific impulse of the propellant, assumed to be 300 s.

On the other hand, for the rideshare option, the mass of propellant needed is assessed by considering the difference between the propellant needed to put ($m_{pload0} + m_{pload}$) into orbit and just putting (m_{pload0}) into orbit:

$$\begin{aligned} m_{propR} = &[(m_s + m_{pload0} + m_{pload})(e^{\left(\frac{\Delta V_{h,i}}{g_0 I_{sp}}\right)} - 1)] \\ &- [(m_s + m_{pload0})(e^{\left(\frac{\Delta V_{h,i}}{g_0 I_{sp}}\right)} - 1)] \end{aligned} \tag{15}$$

Finally, this amount of propellant is translated into dollars using equations 16 and 17 for the dedicated and rideshare launches, respectively:

$$Cost_{dedicated} = 4.26 M\$ + c_p \cdot m_{propD} \tag{16}$$

$$Cost_{rideshare} = c_p \cdot m_{propR} \tag{17}$$

where c_p is the specific cost of propellant, assumed to be 17 \$/kg, the price that NASA was paying for hydrazine by 1990. For the dedicated launch option, an extra cost of 4.26 M\$ is added, which corresponds to the cost of building the rocket specifically for the mission. Since the Rocket Lab's dedicated launch services start roughly at 5 M\$, the cost of building the rocket was assessed by subtracting from 5 M\$ the propellant cost of putting the maximum possible payload (150 kg) in an orbit of 500km and 30 degrees inclination, using the methodology described above. For the rideshare option, on the other hand, since the payload is assumed to be a small fraction of the total launch payload weight ($\alpha = 0.1$, for instance), it is assumed that the cost of building a rocket is assumed by the primary payload.

For a constellation of 6 TROPICS CubeSats, distributed in 3 planes, at 600km altitude and 30 degrees inclination, the total constellation cost estimate by this model is 6.43 M\$ (including satellites and launch costs) and the rideshare option is used. For a constellation of 8 Cyclone Global Navigation Satellite System (CYGNSS) micro satellites distributed in just one plane, the cost estimate is 30.1 M\$ and 2 dedicated launches are chosen since the 8 CYGNSS satellites have a total mass of $8 \times 27.5 = 220$ kg, which exceeds the Electron LV maximum payload mass of roughly 150 kg. Both TROPICS and CYGNSS cost estimates were considered reasonable and consistent with reality. Note that this cost model was used in the TROPICS constellation design study to provide relative cost estimates between constellations rather than accurate absolute cost estimates.

2.3. Robustness / Operational Risk

Another important issue in satellite constellation design is risk of spacecraft and launch vehicle failure, since some constellations may be more robust to operational risks than others. There are many sources of risk for space missions. For instance, the increasing quantity of space debris is a cause of concern since tiny projectiles can damage satellites due to the high collision velocity [24]. This is especially problematic for higher altitudes where the density of the atmosphere is low and atmospheric drag is not capable of removing the abundant small debris. Other common sources of mission failure include communications or power subsystem problems, often due to failure of deployment mechanisms, and launch vehicle failure, leading to complete spacecraft loss in the worst case, or to a reduction in mission lifetime or performance and/or large effort and cost for mission recovery in the best case [25].

Most published work on constellation design [26, 27, 28, 29, 30, 31, 32, 33, 34, 35] focuses on achieving a certain level of performance, usually set by mission requirements, with the nominal constellation, assuming 100 % satellite availability and not taking into account hypothetical spacecraft failures. However, constellations with similar nominal performance may have very different levels of robustness to spacecraft or launch failure, and therefore it is important to consider robustness in constellation design. A simple way to assess constellation robustness is to evaluate if the constellation can still accomplish mission goals and requirements in the event of the loss of one or more spacecraft [36, 37]. Naturally, the smaller the changes in performance after losing spacecraft in the constellation, the larger its robustness –i.e., its capacity to resist coverage degradation. In [38], the degradation of the percent coverage metric is quantified for degraded states of the WILdfire Detection Constellation of nAno saTellites (WILDCAT) of 15 satellites, showing that the total time to achieve 100% coverage notably increases as satellites in the constellation start to fail.

In [12], Ferringer et al. present a framework for the reconfiguration of satellite constellations in the hypothetical case of single-satellite failures by looking at performance, cost and risk

metrics and using the Large-Cluster Epsilon Non-dominated Sorting Genetic Algorithm-II and an *a posteriori* decision support methodology. Focusing on the Global Positioning System (GPS), they solve the reconfiguration problem by optimizing coverage, time of flight of maneuvered satellites, number of maneuvered satellites and propellant consumption (which ultimately is related to the lifetime of the constellation and cost). While this paper considers cost and performance degradation simultaneously, it focuses on optimizing reconfiguration –i.e., maneuvers– as opposed to initial constellation design, and –with the exception, perhaps, of F-Fold Daily Visibility Time (FDVT) if instead of 24 hours, the whole simulation window is considered– on metrics that are mostly relevant to navigation as opposed to Earth observation. FDVT accounts for the total access time during a day period for which at least F satellites in the constellation access a given receiver. This coverage FOM includes some constellation "robustness" information since having multiple satellites accessing a receiver –or a coverage point in our case– is certainly more desirable from a robustness perspective than just having one satellite accessing it, a sufficient requirement in all coverage performance FOMs considered in this paper, as detailed in section 2.1.

In [39], a comparison of cost and performance– or utility– between monolithic and fractionated spacecraft architectures accounting for failure and replacement of spacecraft in the system is done by developing Markov models and running 1-year Monte-Carlo simulations of the models to generate probability distributions of cost and utility metrics. Along similar lines, [40] provides a novel tool to model and quantify the survivability of networks with heterogeneous nodes, specifically applied to space-based networks, to explore the benefits in flexibility and responsiveness of distributing resources across multiple spacecraft with respect to traditional monolithic designs.

In this paper, satellite and launch vehicle failures were modeled as a finite sequence of independent and identically distributed binary random variables– i.e. a Bernoulli process. Each satellite and launch vehicle in the constellation can only take two values to indicate whether the satellite or launch vehicle fail or not before the mission design lifetime. Each variable in the sequence is associated with a Bernoulli trial or experiment. In this study, the probability of launch vehicle failure and satellite failure before the mission lifetime were assumed identical and equal to ($P_f = 0.1$) so the probability of success for each was ($P_s = 1 - P_f = 0.9$). This value of P_f was considered to be conservative with respect to launch vehicle failure and satellite unreliability after successful orbit insertion, according to values found in the literature [41, 42]. Since each satellite and each launch vehicle can either fail or not, and the number of launch vehicles equals the number of planes, there are a total of $2^{n_{sat}+n_{planes}}$ possible states for the system. A brute-force approach was used to calculate the robustness of each constellation, so each of these states was enumerated and evaluated. Specifically, for each state, the probability of being in that state and the corresponding coverage performance were calculated. Given a representation of the state as a bit-string of $N = n_{sat} + n_{planes}$ elements ($X = [x_1, ..., x_N]$), where $x_i = 0$ if element i fails and $x_i = 1$ otherwise, the probability of each state can be computed as follows:

$$P(X) = \prod_{i=1}^{N} P_s^{x_i} \cdot P_f^{1-x_i} = \prod_{i=1}^{N} P_s^{x_i} \cdot (1 - P_s)^{1-x_i} \tag{18}$$

As mentioned earlier, this equation assumes that all satellite and launch vehicle failures are independent. If failures are not independent (e.g., in the presence of common cause failures), then conditional probabilities and the chain rule must be used, and a similar expression can be obtained for certain simplified cases, but this is left out of the scope of this paper.

Note that no new simulations are required to compute degraded coverage performance once the architecture with all its elements has been evaluated. Indeed, if the accesses corresponding to each individual spacecraft in the constellation are stored separately and then merged to calculate the coverage metrics, one can simply choose the subset of accesses corresponding to the satellites that did not fail in that state, merge them, and compute the corresponding coverage metrics. Once probabilities and coverage metrics are available for all possible system states, probability density functions (PDFs) and Cumulative distribution functions (CDFs) for the different coverage metrics can be obtained for the constellation, and the expected coverage performance (mean), the median, or any other percentile of the CDF (i.e., the probability of meeting a certain target value) can be used as a measure of robustness.

2.4. Lifetime

Spacecraft lifetime is another relevant metric to consider in constellation design, especially for satellites in very low orbits (500km or lower), which can suffer from rapid orbital decay due to atmospheric drag. Furthermore, for CubeSats without propulsion subsystems, where orbit maintenance becomes more challenging or impossible, lifetime is a crucial parameter driving mission success. On the other hand, if satellites are placed in higher orbits where drag is negligible, CubeSats without alternative de-orbiting capabilities such as propulsion would orbit almost indefinitely around the Earth after the satellite's mission life, increasing space debris. For that reason, NASA's End of Mission Considerations [43] recommends to set a constellation altitude and area-to-mass ratio so that reentry by atmospheric drag is ensured to occur within 25 years after the end of the mission. Given that for many CubeSats, the operational orbit is unknown until well after the early design phase, this is a challenging requirement. Another important parameter that significantly affects orbital decay besides altitude and area-to-mass ratio is the solar cycle. With increasing solar activity, the atmospheric density and thus drag increase significantly, lowering satellite's lifetime. For that reason, and specially for short space missions, it is relevant to assess the sensitivity of orbital decay to launch date.

While accurate calculation of deorbiting requires numerical propagators, analytical approximations exist that can be used to iteratively calculate mission lifetime. For example, [14] provides the following equations to account for the effect that drag has on satellite decay for circular orbits:

$$\Delta a_{rev} = -2\pi \left(C_D \frac{A}{m} \right) \rho a^2 \tag{19}$$

$$\Delta P_{rev} = -6\pi^2 \left(C_D \frac{A}{m} \right) \rho a^2 / V \tag{20}$$

where Δa_{rev} and ΔP_{rev} are the changes in semi-major axis and orbital period respectively per revolution (orbit). C_D is the dimension-less drag coefficient of the satellite, A is the cross-sectional area (perpendicular to the velocity vector), m is the satellite mass, a is the current semi-major axis, V is the current satellite velocity and ρ is the current atmospheric density, which as mentioned is very sensitive to altitude and solar activity. Note that both V and ρ depend on altitude and thus on a. Using these two equations iteratively, an estimation of satellite lifetime can be assessed by observing the changes in altitude, orbital period and satellite velocity in time. However, in this paper, all lifetime calculations have been performed propagating the spacecraft using a high precision propagator available in Orekit, keeping track of its semi-major axis and stopping the propagation at an altitude equal or lower than 120 km. This approach, despite being more computationally expensive, allows us to take into account other aspects such as oblateness of the Earth and use the sophisticated density models available in the Orekit software library.

2.5. Deployment

As mentioned in section 2.2, often small satellites must be launched as secondary payloads due to budget constraints. This fact sometimes restricts their deployment in the required/ideal constellation geometry [44]. For example, even separation of satellites in mean anomaly within a plane and even separation in RAAN across planes are usually desirable to minimize long gaps, but instead of that, a secondary launch may mean reduced or no separation within or across planes. In [45], Fakoor et al. develop a new approach for satellite constellation reconfiguration based on Lambert's theorem that minimizes fuel cost and takes into consideration risk issues such as collision avoidance between satellites. For small satellites without propulsion capabilities, drag-based deployment strategies are typically considered to reach some level of spacing between satellites [46, 47, 48, 49, 50, 51]. These strategies make use of the ability to change the geometry of the spacecraft through attitude maneuvers or deployables such as solar panels to change the drag of each individual spacecraft, which can then be used to adjust their relative phasing. These strategies have been demonstrated on orbit by the CYGNSS mission. CYGNSS consists of 8 microsatellites which, once deployed by a single launch vehicle in a 500km altitude orbit, were evenly spaced in mean anomaly (45 degrees from each other) in the same orbit using a differential drag technique [52]. A similar approach was studied for TROPICS and is described in Section 4. Of particular interest is the time required to reach the desired constellation geometry (e.g., even separation in mean anomaly), as this can be an important fraction of the mission lifetime. This metric– which we called time to operational orbit– is significant, since some deployment strategies can take years to complete, limiting mission operational lifetime.

Time to operational orbit can be estimated analytically using equations 19 and 20 provided in subsection 2.4. Indeed, an analytical estimate of the variation of altitude and orbital period per revolution for the different satellites placed in the same orbital plane can be obtained. Next, using the difference in orbital period between a pair of satellites, it is possible to keep track of their relative mean anomaly variation per revolution. However, similarly to what was done for lifetime computations, this analytical approach was not used in this study and, instead, numerical propagation of the different satellites was used to keep track of the separation of satellites during mission deployment.

3. Setting up simulations for coverage calculations

Fast analytic approximations for evaluating Earth coverage are available for several parameters such as Footprint Area (FA), which is "the area that a specific instrument or antenna is viewing at any instant" [14], Instantaneous Access Area (IAA), which is "all the area that the instrument or antenna could potentially see at any instant" [14], Area Coverage Rate (ACR), which is "the rate at which the instrument or antenna is sensing or accessing new land" [14], or Area Access Rate (AAR), which defines "the rate at which new land is coming into the spacecraft's access area" [14]. However, these approximation models do not include aspects such as the oblateness of the earth, the rotation of the Earth underneath the satellite orbit, orbit eccentricity, or the assessment of coverage by more than just a single satellite. These analytic approximations were not used in this work and, instead, numerical simulation was performed to compute the different metrics listed in subsection 2.1, which are not assessed by any analytical model.

Some of the main issues to take into account when setting up a coverage analysis simulation are:

- **The number and the distribution of the points in the coverage grid.** The greater the number of points, the better the spatial resolution of the results but, the longer the simulation time. Also, failing to choose an adequate distribution of the grid points may lead to biased results. For instance, creating a grid with constant granularity in both latitude and longitude degrees would place many more points per unit surface area in the poles than near the equator.

- **The simulation time.** It must be long enough to at least capture several orbits of the different satellites, the repeat period of a repeat ground track orbit, and ideally any relevant seasonal effects, so that the results obtained are representative of the whole mission life.

- **The time step of the propagation.** It should be a small fraction of the orbital period, and it should be selected together with the coverage grid resolution and the sensor field of view. Specifically, the time step should be chosen so that there are no spatial gaps in sensor footprint between two consecutive time steps, since that could lead to artificially missing grid point accesses.

- **Fidelity of the propagation.** The simulations can be run using models of various complexity and fidelity. Logically, the more complex the model, the longer the simulation time. For satellite propagation, Keplerian, J2, and high-precision numerical models can be considered. The Keplerian propagator only takes into account the symmetric central body force. The J2 propagator adds to that first model the J2 zonal harmonic coefficient contribution to account for Earth's oblateness, which allows to model sun-synchronous orbits among other things. Finally, high precision numerical propagators incorporate J2 effects, drag, third-body effects of the Sun and the Moon, and solar radiation pressure disturbances to the propagation of the satellite.

4. Application to TROPICS mission

This section describes the process followed to explore various constellation design alternatives for the TROPICS mission, using the FOMs introduced in section 2.

4.1. Simulation parameters

All the simulations performed in this paper were run using Orekit, an open-source space dynamics library written in Java that provides basic tools and accurate and efficient low-level components for the development of flight dynamics applications. On top of the Orekit library, we built the capability to run coverage analysis for the different purposes of this work. Our code is open source and can be downloaded from GitHub [53]. The main parameters considered when setting up the coverage analysis for the TROPICS mission are the following:

- A grid of 9° granularity in latitude, resulting in a grid of 512 points around the Earth surface. Moreover, the number of points at each latitude has been chosen to be proportional to the cosine of the latitude to obtain equal horizontal distances between points. Therefore, fewer points are placed in higher latitudes to avoid statistically weighting more the poles in the global coverage metrics. This is especially relevant for the TROPICS mission, which focuses on keeping track of storms in the tropical regions.
- The simulation time for each scenario was set to 1 week, enough to capture about 100 orbital periods for the highest orbits considered of 800km (which corresponds to about 109 orbital periods at 400km). Clearly, one week is not enough to capture seasonal effects. Specifically, the seasonal effects that are most relevant to this problem are variations on atmospheric drag due to the solar cycle that change coverage metrics. After performing a few simulations with a 1 year duration and comparing the results with the ones obtained with just 1 week long simulations, the biggest differences in coverage metrics (revisit times, response times and CHRC statistics) were found to be around 20% for constellations at 400km (where drag is very large) and 5% or lower for altitudes of 600km or higher, which was judged acceptable for Pre-Phase A studies.
- A rectangular field of view (FOV) was used to model the imaging concept of the payload. The TROPICS payload is a high-performance radiometer that rotates about the velocity vector at 30 rpm and it has a beamwidth range from 1.5° to 3.0°. The rectangular FOV used in this paper is an approximation of TROPICS' payload characteristics: the cross-track FOV was set to the max value in terms of incidence angle for observations (57°), and the along track FOV was set together with the simulation time step and the spacing between points in the Earth grid so that no gaps were artificially generated in the along-track direction (20°).
- We used a high precision numerical propagator that incorporates J2 effects, drag (DTM2000 atmospheric model [54]), third body effects of the Sun and Moon, and solar radiation pressure disturbances to the propagation of the satellite. A satellite mass of 6kg, a solar area of $0.058m^2$ and a nominal drag area of $0.075m^2$ were used to model the TROPICS CubeSat.

4.2. Coverage Tradespace Exploration

The main decisions defining the TROPICS constellation tradespace were the total number of satellites, the number of planes, and the orbit altitude and inclination. All 4400 circular Walker constellations consisting of up to 16 satellites, and including altitudes of 400km, 500km, 600km, 700km and 800km, and inclinations of 30°, 51.6° (the ISS inclination, because there are many launch opportunities to that orbit), 90°, and Sun-Synchronous Orbits (SSO) were simulated. Hybrid constellations with satellites at different altitudes and/or inclinations were not considered since mission operations, maintenance and data processing would get more complicated. Nevertheless, 100 random hybrid constellations containing multiple planes equally spaced in RAAN at different altitudes and inclinations were simulated to assess whether better coverage performance and cost could be achieved by going beyond Walker constellations. Satellites within the same plane were equally spaced in mean anomaly to perform a fair comparison with Walker constellations. All 100 hybrid architectures were dominated by the Pareto front of the 4400 Walker constellations except for one hybrid constellation, which appeared to be in the combined Pareto front. However, this hybrid architecture was only 34$ cheaper than another Walker constellation that offered 19 minutes better mean revisit time, and 122$ cheaper than another walker constellation that offered 33 minutes better mean response time. This cost difference is very minor and it is clearly outweighed by the increase of operational costs when those are taken into consideration. Therefore, we concluded that restricting our design space to only Walker constellations was a reasonable assumption for our problem.

In order to select the 'preferred' constellation for the TROPICS mission based on the dataset resulting from those simulations, we analyze the independent impact of each decision variable on coverage performance in a more linear or sequential way than the one followed in reality, but the main arguments from the actual process are all present. We start by exploring

the effects of inclination on the main goal of the TROPICS mission, which is to monitor hurricanes and storms located in lower latitudes. Results show that, when looking at aggregate coverage metrics, choosing the appropriate inclination has the largest effect on accessing certain latitudes, so a preliminary value of inclination can be chosen at this state. Next, exploring the effect of altitude leads to a preliminary altitude decision made as a compromise between spatial resolution, coverage performance, lifetime, and cost. Once both inclination and altitude are set, the number of satellites in the constellation is chosen to meet the mission's coverage performance threshold while minimizing cost and considering constellation robustness to hypothetical failures. Finally, the number of planes decision is evaluated to optimize the constellation's response time and minimizing the longest gaps of coverage while subject to the constraint of having a maximum of three launches.

In order to study the trades between the different constellations simulated, different coverage and performance metrics were considered: weighted mean revisit time, weighted median revisit time, weighted 90th percentile of revisit time, weighted maximum gap time, weighted mean response time, weighted CHRC and cost. All metrics were latitude-weighted using the information presented in Figure 3 from Section 2. For constellations with inclination of 30°, the weights corresponding to the latitudes larger than 36° were set to 0. The reason behind this modification is that, even though the weights were already very small (a total contribution of 0.425% to the aggregated coverage metrics), at this field of view, higher latitudes are not reachable from 30° inclination constellations and the weighted average of the different metrics was significantly affected by gaps of non-accessed latitudes, whose length was the entire simulation time.

Additionally, another important metric to consider was the instrument spatial resolution SR, which for a microwave radiometer with a circular aperture is given by:

$$SR = 1.22\frac{\lambda}{D}r \quad [1] \tag{21}$$

where r is the range or distance between the instrument and the Earth grid point, which for circular orbits is roughly equal to the altitude divided by the cosine of the off-nadir look angle η, $r = h/cos(\eta)$, and λ and D are the wavelength and aperture of the instrument, respectively. Note that this is the SR corresponding to the azimuth direction (perpendicular to the range direction) –there is another $1/cos(\eta)$ for the range direction. The first portion of the TROPICS radiometer payload uses eight channels uniformly spaced in frequency from approximately 114 to 119GHz and one window channel at 108-109GHz. The instrument has a single aperture of approximately 7cm (the actual aperture is 8.3cm but the reflector is under-illuminated to reduce sidelobes) [55], which leads to different values of spatial resolution for the different channels. A requirement for the TROPICS mission is to have a ground spatial resolution of 25 km averaged over the entire swath.

Whereas high altitudes and high numbers of satellites are preferred from a coverage perspective, the cost and spatial resolution metrics will penalize these architectures, thus establishing a basic trade-off.

Figure 4 shows a box-plot comparison of the latitude-weighted mean, median, 90th percentile and maximum revisit times for the different inclination groups considering the 940 constellations with 3 or fewer planes out of the 4400 Walker constellations simulated. Note that in each of these boxplots, there are 235 constellations with different values of altitude, number of satellites, and number of planes. The 30° inclination architectures provide significantly better coverage for the tropical regions, going from a weighted mean revisit time mean of 101 minutes for SSO to 45 minutes for 30°.

Mean revisit time and high percentiles of revisit times are the metrics that change the most when varying the inclination of the orbits, whereas the weighted median revisit time is not very sensitive to inclination changes. These results are also exemplified in Figure 5, where we plot the CDFs of 4 specific constellations out of the simulated Walker constellations, all with 12 satellites distributed in 3 planes and 600km altitude (the values that were eventually recommended as the baseline architecture) but inclinations of 30° , 51.6°, 90° and SSO respectively. All curves show similar values of median revisit time and low percentiles of revisit times but they diverge significantly in the higher percentiles of revisit times. Thus, all the architectures with $i \neq 30°$ were filtered and ruled out for further analysis as they are more costly and do not provide any better coverage performance in this problem than the 30° ones.

Figure 6 shows weighted mean revisit time with respect to mission cost for all the architectures with 30° inclination. Five different curves corresponding to the different altitude cases can be distinguished. As expected, satellites in higher altitudes offer better mean revisit time values; at the same time, these architectures have worse spatial resolution and are more expensive since the launch cost grows with altitude. Therefore, architectures at 600km offer a good trade between cost, coverage performance and spatial resolution. This trade-off can be also observed in Figure 7, showing the non-dominated volume containing all simulated Walker constellations with 3 or fewer planes with their associated values of cost, weighted mean revisit time (or coverage performance) and spatial resolution. Going from an altitude of 400km to 600km, we significantly decrease the weighted mean revisit time. Moreover, the coverage performance at 600km is good enough for the mission purposes as we can easily get weighted mean revisit times of less than 60 minutes and, increasing the altitude of the architecture would worsen both cost and spatial resolution. In addition, the 600km altitude is high enough to avoid an exceedingly short mission lifetime due to drag, but still low enough to be able to satisfy NASA's recommendation to deorbit within 25 years of the end-of-life.

With a 30° inclination and 600km altitude selected, the num-

[1] This spatial resolution formula neglects Earth curvature. A more exact expression is $SR = R_E \cdot (\alpha_2 - \alpha_1)$ where $\alpha_{1,2} = 90 - \eta_{1,2} - \epsilon_{1,2}$, $cos(\epsilon_{1,2}) = \left(\frac{R_E+H}{R_E}\right) sin(\eta_{1,2})$ and $\eta_{1,2} = \eta \pm 1.22\frac{\lambda}{D}$. R_E is the Earth radius, H is the altitude, η is the instrument off-nadir look angle, ϵ is the spacecraft elevation angle, and α is the Earth central angle measured at the center of the Earth between the intersection points of Earth surface and nadir, and Earth surface and the instrument field of view center axis, respectively.

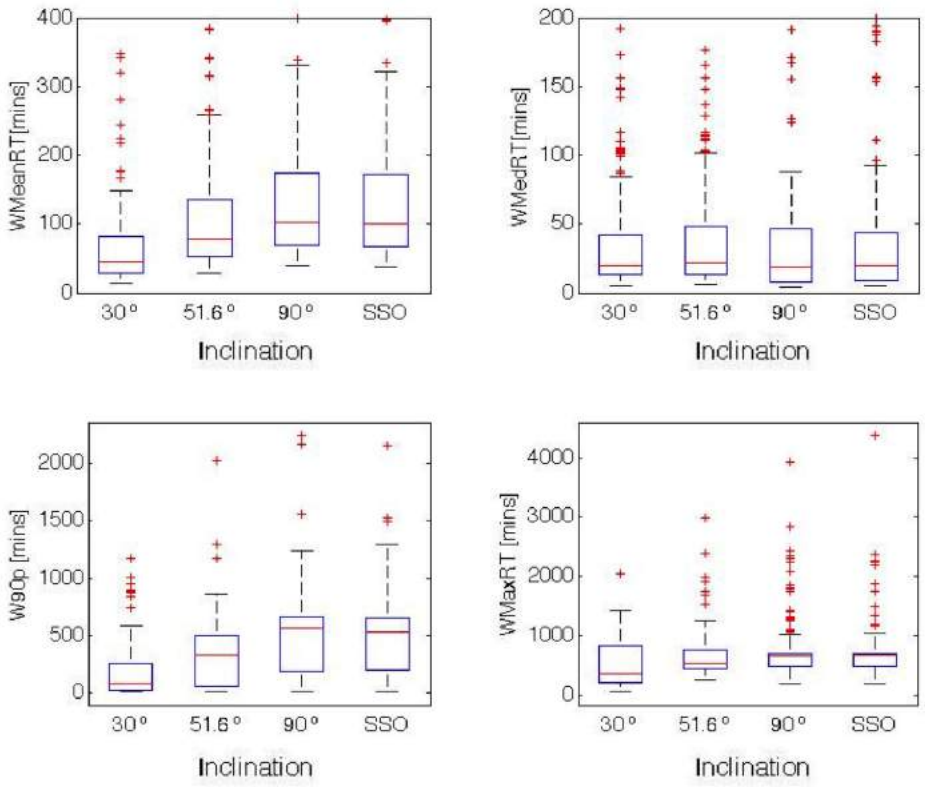

Figure 4: Comparison of the latitude weighted mean, median, 90th percentile and maximum revisit time for the different inclinations of study

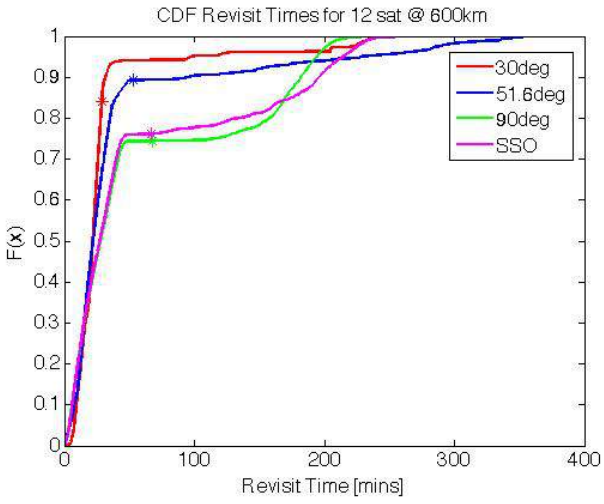

Figure 5: Comparison of the CDFs of 4 Walker constellations of 12 satellites at 600km altitude and different inclinations. The markers (*) show the values of weighted mean revisit time for each of the four configurations.

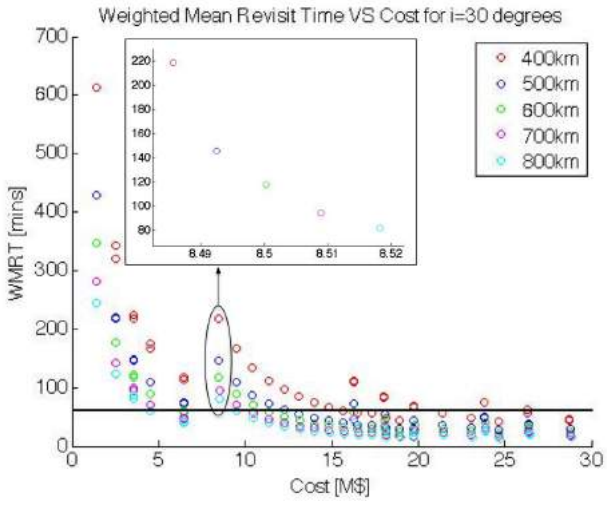

Figure 6: Latitude-weighted mean revisit time vs cost for all 30 degrees simulated constellations. The black horizontal line corresponds to the 60 minute weighted mean revisit time requirement. Constellations of 400 km, 500 km, 600 km, 700 km and 800 km have a spatial resolution in the 183 GHz band of 11.43 km, 14.29 km, 17.14 km, 20 km and 22.86 km respectively.

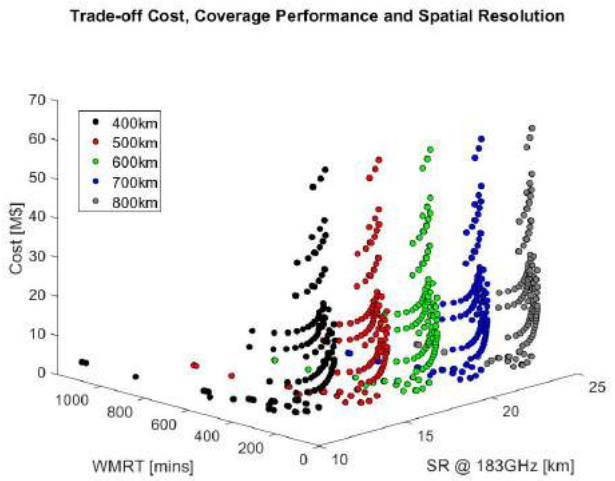

Figure 7: Non-dominated volume showing cost, weighted mean revisit time and spatial resolution in the 183 GHz band for all simulated Walker constellations with 3 or less planes

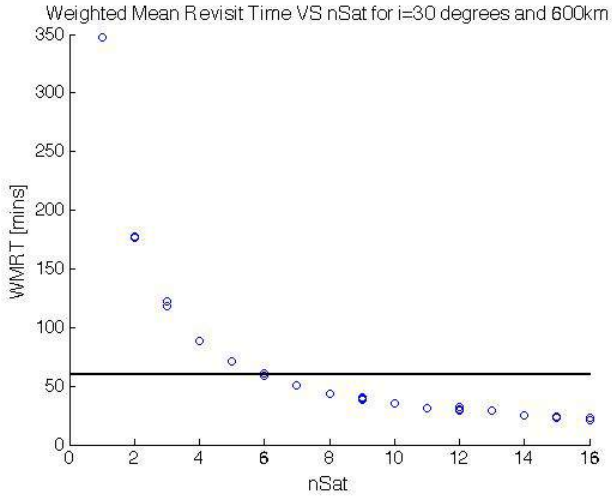

Figure 8: Latitude-weighted mean revisit time vs nsat for all constellations with 30° inclination and 600km altitude

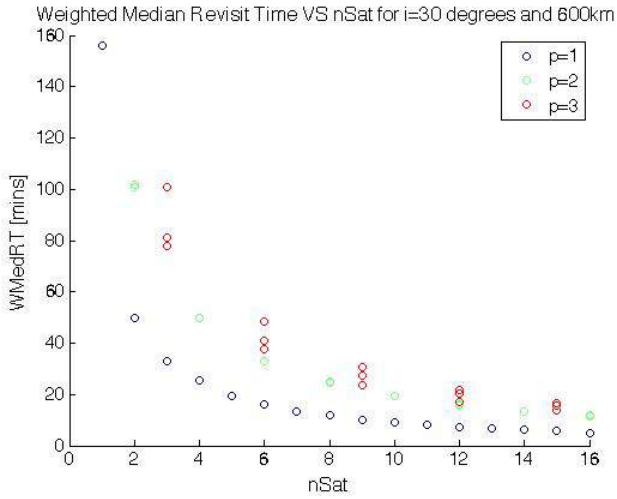

Figure 9: Latitude-weighted median revisit time vs nsat for all constellations with 30° inclination and 600km altitude

ber of satellites in the TROPICS constellation and the number of planes in which to distribute the satellites were the following design decisions to make. In Figures 8 and 9, the number of satellites required to achieve certain values of weighted mean and median revisit times can be obtained, respectively. However, increasing the number of satellites will also increase cost, as expected and seen in Figure 10. Therefore, the minimum required number of satellites will be selected unless risk/robustness factors are considered. In other words, a more robust constellation design may be considered to account for hypothetical satellite losses that would potentially decrease coverage performance. For this reason, at this point in our constellation tradespace analysis, we decided to consider two different candidate constellations:

- Threshold architecture, formed by 6 satellites, which allows us to meet the main mission coverage requirement to have a weighted mean revisit time equal or less than 60 minutes with the lowest number of satellites possible. Figure 8 shows that with 6 satellites, we obtain a weighted mean revisit time of 59 mins (right below the 60-min requirement).
- Baseline architecture, formed by 12 satellites, which not only allows us to meet the mission coverage requirements in the nominal case (weighted mean revisit time goes down to 29 mins) but also in degraded cases with a hypothetical LV failure or several satellites losses, as it will be shown later in this section. Moreover, the baseline architecture meets the Observing Systems Capability Analysis and Review Tool (OSCAR) Observing Cycle requirement of 30 minutes for the measurement of several physical variables in applications related to weather, water and climate such as precipitation type and intensity; air pressure, temperature and specific humidity in surface; and vertical and horizontal wind speeds over the Earth surface[56].

Finally, the impact in coverage metrics and gap time distributions of choosing one vs several planes in which to distribute all the satellites was assessed. It was found that median and high percentiles of revisit times are the metrics that change the most when varying the number of planes, whereas the weighted mean revisit time is barely affected. These results are illustrated in 2 plots: Figure 11 shows a comparison of the CDFs of 3 different architectures, all with 12 satellites at 600km altitude and 30° inclination distributed in 1, 2 and 3 planes (local analysis). In Figure 12, weighted mean, median, maximum and 98th percentile gaps are compared for different number of planes including all constellations at 600km and 30° inclination (global analysis). Both the global and local analysis suggest that median and lower percentiles of revisit times appear to be slightly better for architectures of one plane whereas higher percentiles (i.e., longest gaps) are much shorter in architectures with 3 planes. This happens for 2 reasons:

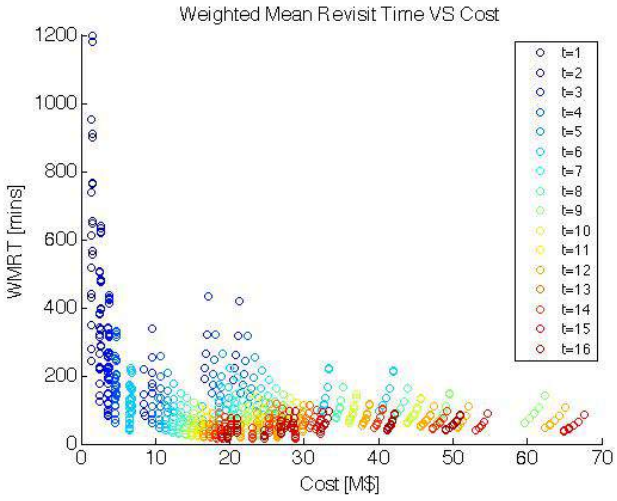

Figure 10: Latitude-weighted mean revisit time vs cost for all constellations

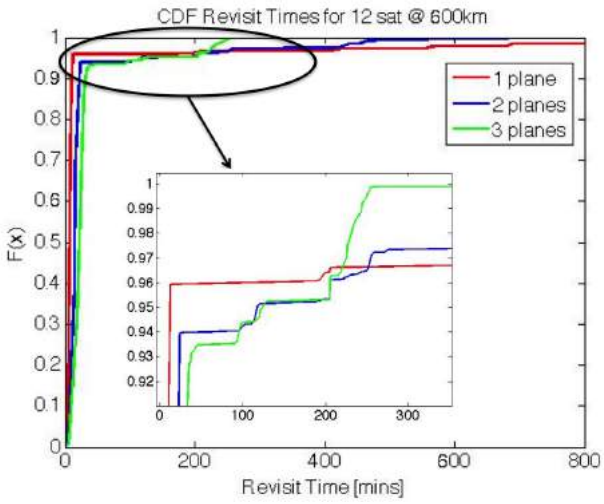

Figure 11: Comparison of the CDFs of 3 Walker constellations of 12 satellites at 600km altitude and 30 degrees inclination for p = 1, 2 and 3

- As discussed earlier, the revisit times CDFs in constellations with just one plane show many short accesses (hence the low low percentiles or even low median if there are many satellites and thus many short gaps) but also very long gaps (hence high high percentiles). Distributing the satellites in several planes makes the short gaps a bit longer (higher low percentiles) while making the long gaps significantly shorter (lower high percentiles).
- The variability in total number of gaps in different scenarios can significantly affect all the revisit time statistics in the CDF.

Moreover, two very sensitive metrics to the selected number of planes are mean response time and the continuous high revisit coverage (CHRC). As it was mentioned in Section 2, the former is by definition the average time from when we receive a random request to observe a point until we can actually observe it, and the latter is the percentage of time where the grid point is either in an access or in a gap shorter than a certain threshold, set in our case to 2 hours. In Figures 13 and 14 we can see that distributing the satellites in more than one plane, the time that the constellation will take to access a point after a random request will be shorter than if the satellites were put in a single plane. Likewise, in architectures with just one plane, there is a larger fraction of gaps longer than 2 hours compared to the scenarios where the satellites are distributed in 2 or 3 planes.

Another factor analyzed was the influence of the number of planes on cost. The two plots in Figure 15 show mean revisit time against cost for all Walker constellations with 600km altitude, 30° inclination and less than 4 planes. The plot on the left color-codes the different architectures by type of launch (i.e., rideshare or dedicated) and the one on the right by number of planes. With $\alpha = 0.1$ (i.e., for the rideshare option, the TROPICS payload weight per launch vehicle is limited by the 10% of the maximum payload weight supported by the Electron launch vehicle), only roughly 25% of all Walker constellations with 3 or fewer planes use the rideshare option. The reason behind this fact is that most constellations with large n_{sat}/n_{planes} ratio need to use the dedicated launch option since the TROPICS payload per launch exceeds the 10% of maximum payload weight. Therefore, distributing the satellites in several planes could help decrease launch vehicle cost by making the rideshare launch feasible. For instance, the configuration with six satellites and one plane has a cost of M11.37 and the TROPICS threshold configuration with six satellites distributed in 3 planes has a cost of M6.43. That being said, the TROPICS mission probably will not use rideshares since those launch services are not available at a destination orbit of 30° inclination. Instead, NASA will buy n_{planes}–potentially 3– dedicated launches, adding a substantial overhead in launch cost.

Given that the only requirement set by the TROPICS mission in terms of launch vehicle is to use at most 3 launches (i.e., 3 planes), distributing the constellation satellites in more than one plane was ultimately recommended to shorten the long gaps and get more desirable revisit times CDFs, as well as mean response time and CHRC values. Furthermore, as it will be detailed later in the section, distributing the satellites in 3 planes

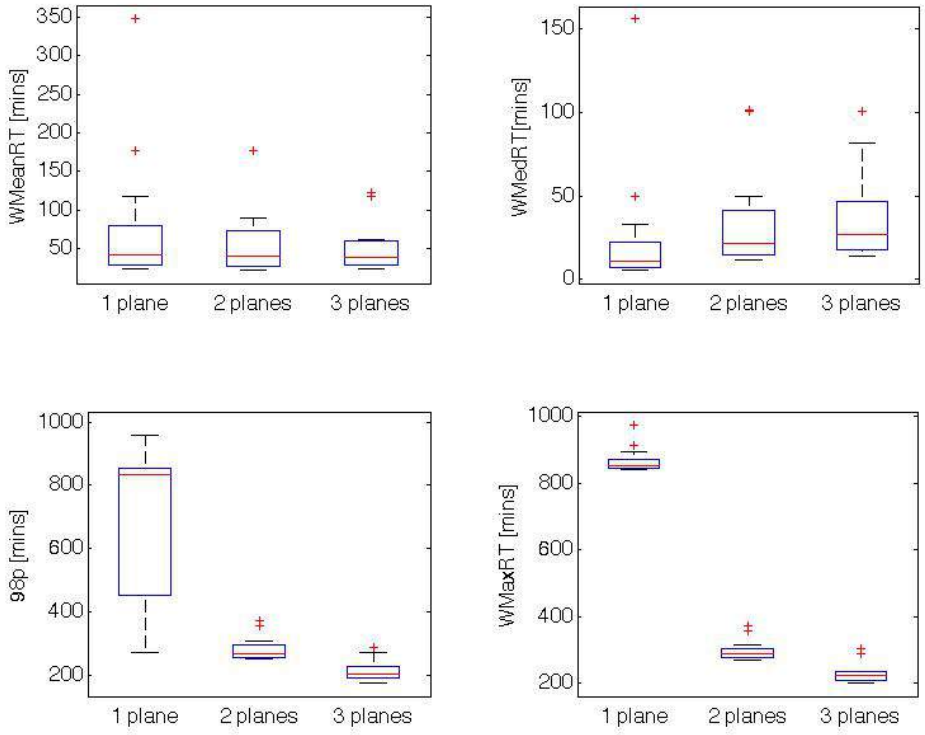

Figure 12: Comparison of the latitude-weighted mean, median, 98th percentile and maximum revisit time for different number of planes including all constellations with 30 inclination and 600km altitude

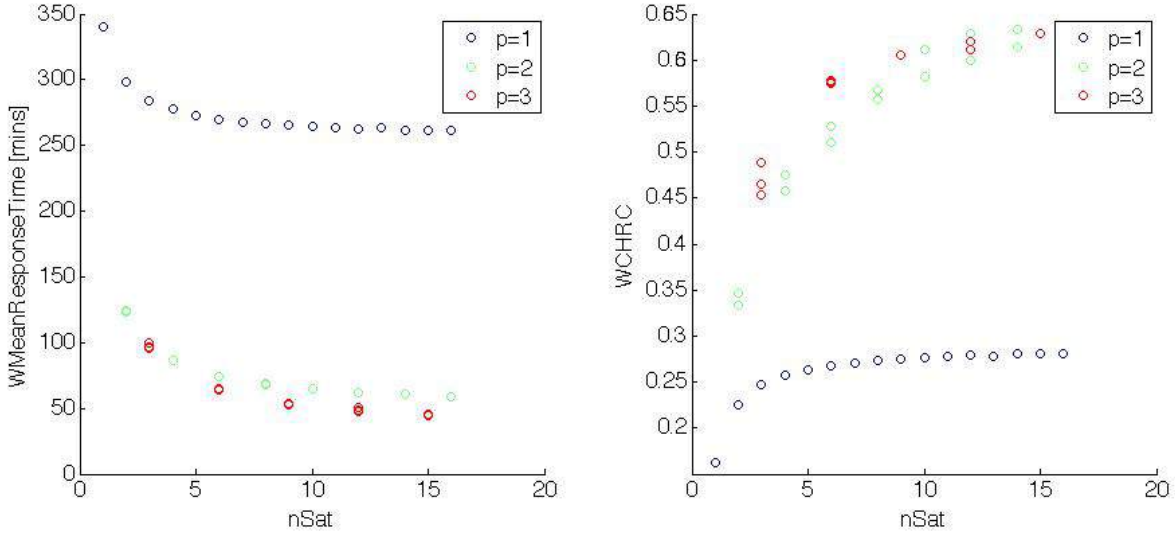

Figure 13: Latitude-weighted mean response time and Latitude-weighted CHRC_120mins vs nsat for all constellations with 30° inclination and 600km altitude

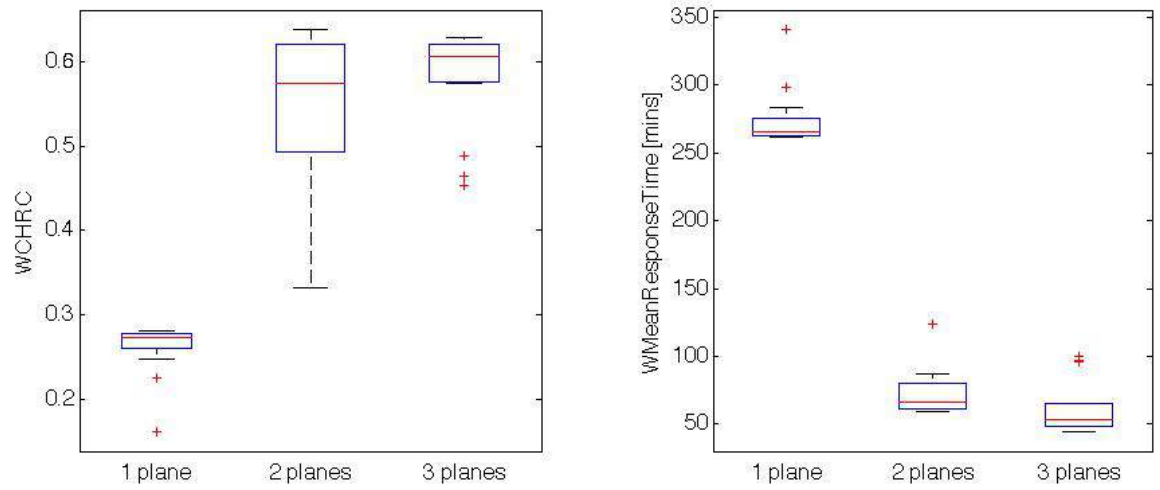

Figure 14: Comparison of the latitude-weighted CHRC_120mins and mean response time for different number of planes including all constellations with 30° inclination and 600km altitude

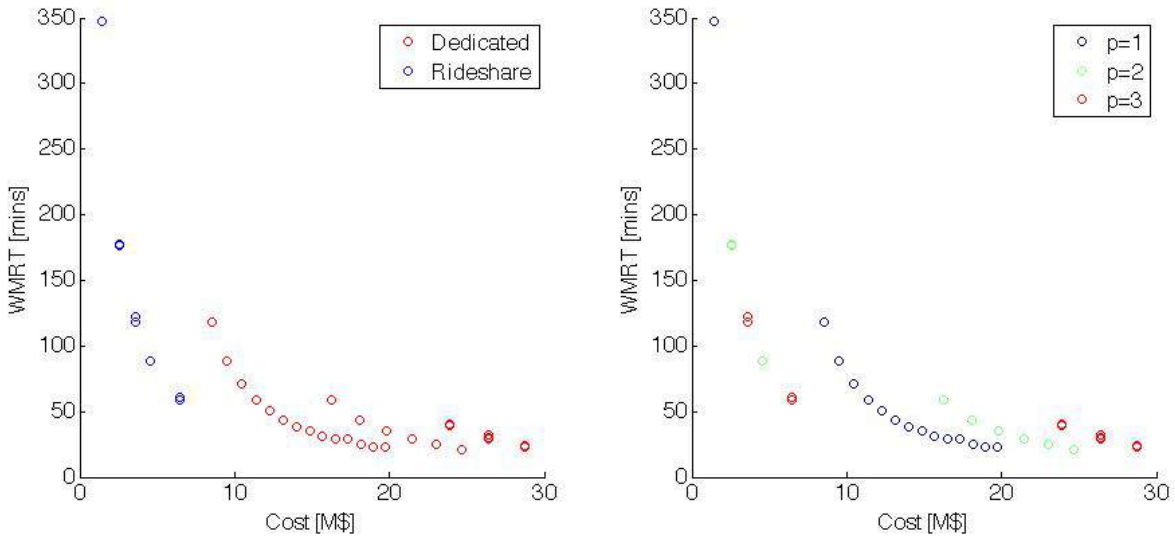

Figure 15: Mean revisit time vs cost for all constellations with 30° inclination and 600km altitude

provides better coverage performance robustness to LV failures than placing the satellites in just two planes.

As shown in Figure 16, the second mission coverage requirement of having a mean revisit time (unweighted, since we are showing the metric for different latitudes) of 60 minutes or less in the tropics regions is well accomplished by the suggested TROPICS baseline constellation, consisting of 12 satellites distributed in either 2 or 3 different planes equally spaced in RAAN at 600 km and 30° inclination. However, the mean response time metric is significantly better in the 3-plane constellation.

4.3. Robustness Characterization

The model described in Section 2 to assess robustness of coverage performance to spacecraft and launch vehicle failure was applied to the TROPICS case study. It is worthwhile mentioning that many states enumerated by the brute force approach are not unique –they are equivalent due to symmetries. For example, since all planes are evenly spaced in RAAN, the 4-4-3 configuration[2] is equivalent to the 3-4-4 and 4-3-4 configuration. In other words, the 4-4-3 configuration can have 4×3 different states depending on which of the 12 satellites fails, but these 12 states all have the same performance metrics due to symmetry. The degradation of coverage performance metrics due to successive satellite losses is illustrated in Figure 17, starting from

[2]In this notation, planes are separated by a dash and each digit corresponds to the number of satellites in a specific plane. For instance, in the 4-4-3 configuration, there are 3 planes with 4, 4 and 3 satellites, respectively. Note that in the x-axes of Figures 17, 18 and 19, the - are omitted to improve readability.

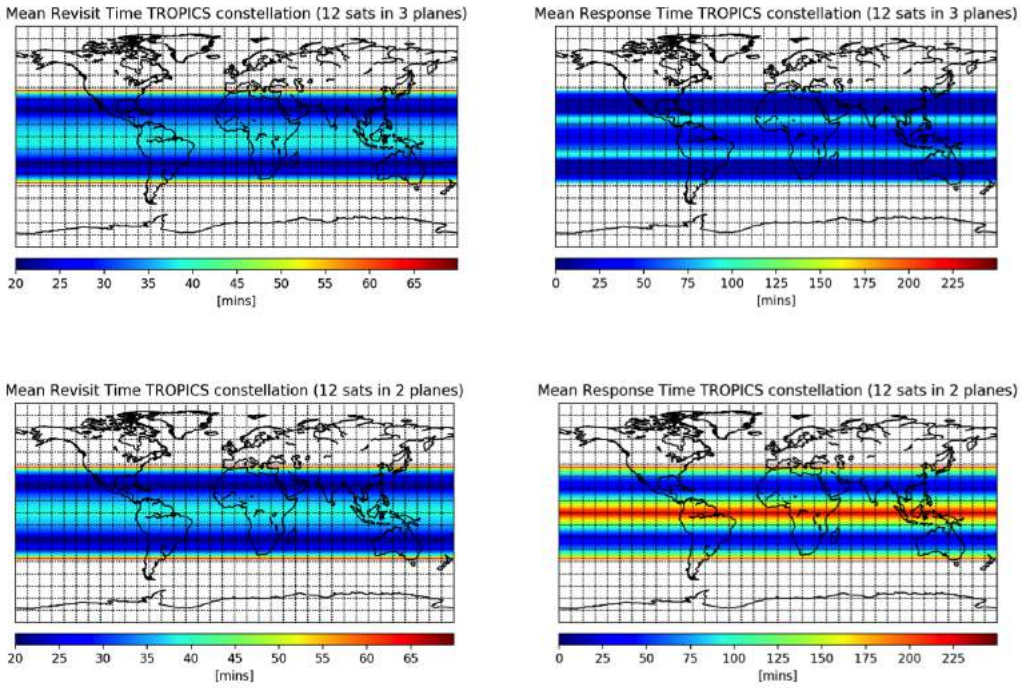

Figure 16: Mean revisit time and mean response time heat maps of the baseline constellation of 12 satellites distributed in 3 planes or 2 planes at 600km altitude and 30° inclination

the baseline architecture with a total number of 12 satellites distributed in 2 or 3 planes. Similarly, Figures 18 and 19 capture the effect of launch vehicle failure on coverage performance for both baseline– i.e. 12 satellites– and threshold– i.e. 6 satellites– architectures. In these figures, each point corresponds to just one of the several different possible states for that configuration and it is just a way of visualizing some of the most relevant coverage metrics degradation information. As observed in the boxplots from Figure 17, differences were found to be small, so the chosen states for each configuration were found to be representative of all the other different possible states of that particular configuration.

Starting from two constellations of 12 satellites, distributed in 2 and 3 planes equally spaced in RAAN respectively, the degradation of the different coverage metrics is observable with successive satellite losses in the different planes. Note that the planes are indistinguishable from one another since they have identical altitude and inclination values and they are evenly distributed in RAAN. We can notice a significant jump in performance (performance plateaus are often present in constellation design [38, 14]) for the transition from a 2-3-3 to a 2-2-3 configuration in the 90th percentile of revisit times. The degradation becomes noteworthy for small constellations with only 5 or 6 satellites, for which any satellite loss implies a significant reduction of coverage performance, especially for the higher percentiles of the gap statistics. Moreover, even though mean revisit times of less than 60 minutes can be achieved by the threshold configuration with only 6 satellites (seen both in Figures 8 and 17), we can conclude that the 6-satellite configuration is not resilient to even a single satellite loss, since the weighted mean revisit time would go from 59.06 mins to 70.89 mins for the 2-2-2 configuration and from 58.55 mins to 70.4 mins for the 3-3 configuration. On the other hand, using the baseline configuration with 12 satellites, the requirement of having a weighted mean revisit time of less than 1 hour can still be met even when six satellites are lost. Similarly, a launch vehicle failure would imply losing an entire orbital plane. Therefore, metrics that are sensitive to the number of planes, such as mean response time and higher percentiles are again the most impacted, as seen in Figures 18 and 19. We can also conclude that the baseline configuration distributed in 3 planes (4-4-4), which has a value of mean revisit time of 29.66 minutes, is resilient to a launch failure and two additional satellite losses, since the 4-4-0 and 3-3-0 configurations have weighted mean revisit time values of 44.37 min and 58.55 min, respectively. On the other hand, it is shown that the baseline configuration distributed in 2 planes (6-6), which has a value of mean revisit time of 28.91 minutes, is somewhat resilient to a launch vehicle failure since the weighted mean revisit time for the 6-0 configuration is 58.74 min, but the higher percentiles of the gap statistics together with the metrics of mean response time and CHRC would significantly worsen with the resulting 1-plane constellation. Also, the 6-0 configuration does not allow any additional satellite loss to meet the TROPICS mission requirement. Fi-

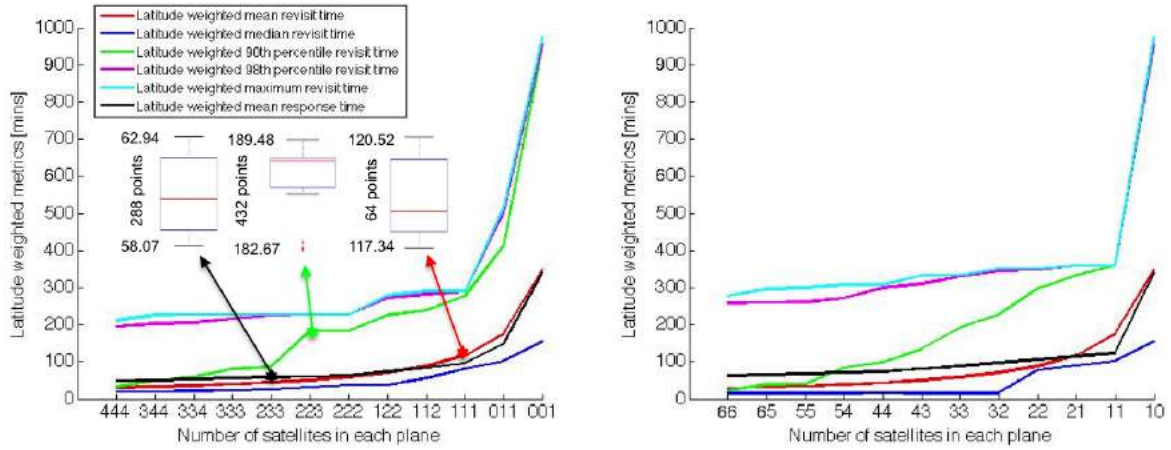

Figure 17: Degradation of the latitude-weighted metrics due to satellite losses for constellations of 12 satellites distributed in 3 and 2 planes respectively and equally spaced in RAAN at 30° inclination and 600km altitude

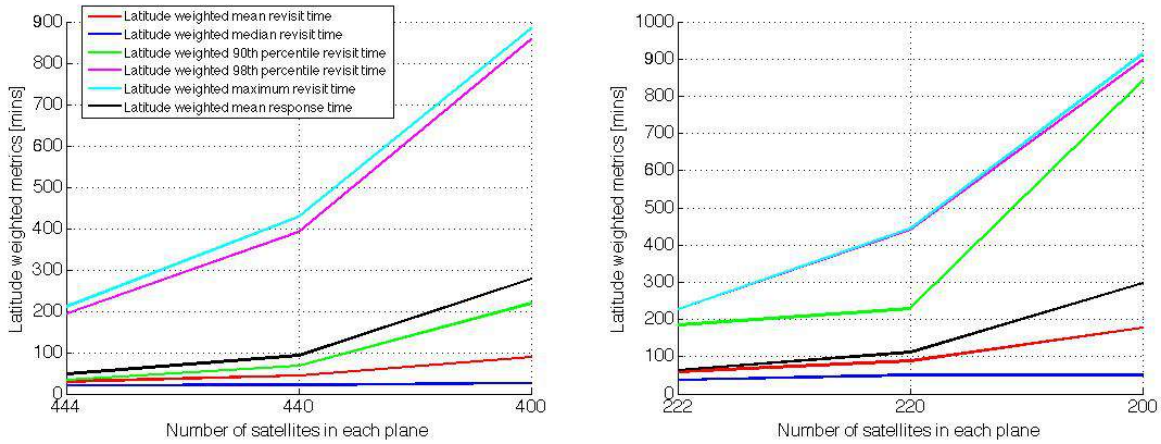

Figure 18: Degradation of the latitude-weighted metrics due to launch vehicle failure for the baseline and threshold architectures with the satellites distributed in 3 planes equally spaced in RAAN at 30° inclination and 600km altitude

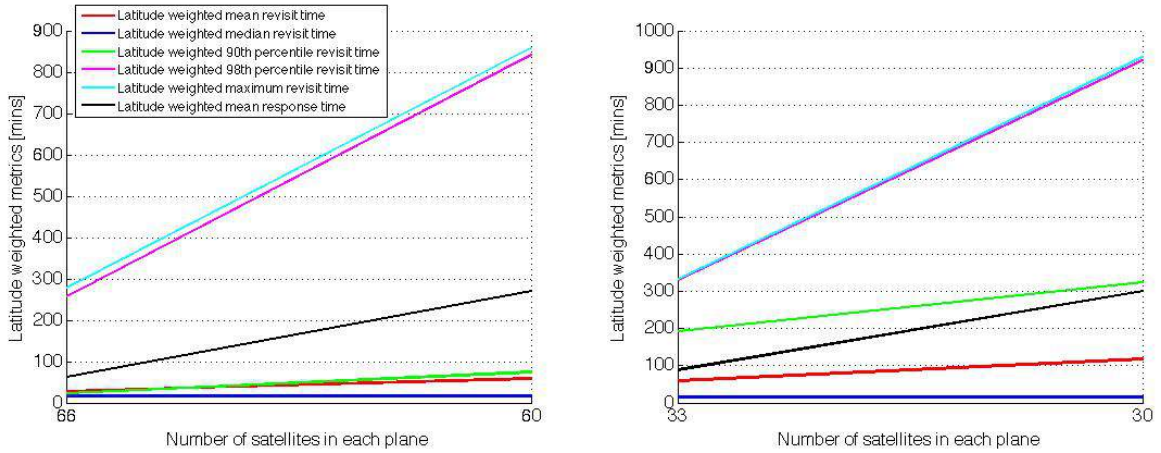

Figure 19: Degradation of the latitude-weighted metrics due to launch vehicle failure for the baseline and threshold architectures with the satellites distributed in 2 planes equally spaced in RAAN at 30 deg inclination and 600km altitude

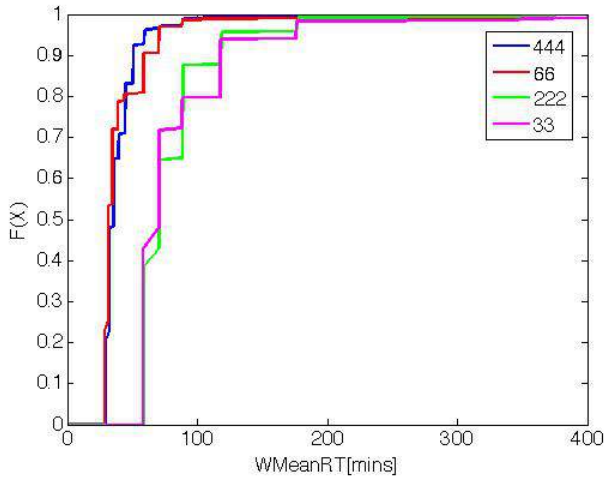

Figure 20: Cumulative Distribution Function of weighted mean revisit time for the 4-4-4, 6-6, 2-2-2 and 3-3 constellations at 30° inclination and 600km altitude

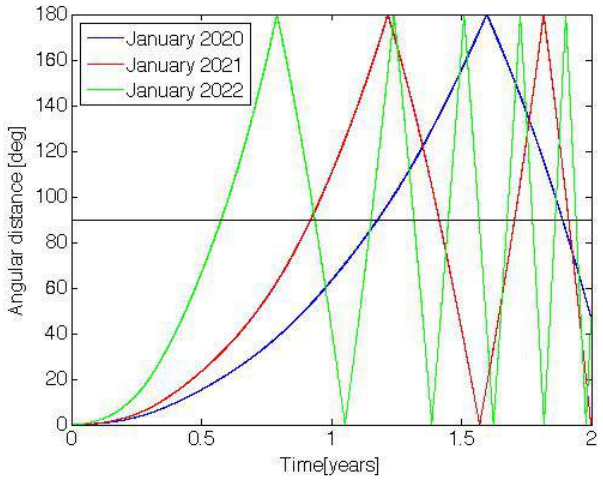

Figure 21: Angular separation over time between high drag and low drag satellites at 30° inclination and 600km altitude for the described deployment strategy

nally, as mentioned previously, threshold configurations (2-2-2 and 3-3) are not resilient to a single satellite loss and, therefore, neither are they to a launch failure, which would imply the loss of more than 1 satellite.

The $2^{n_{sat}+n_{planes}}$ different states were enumerated by brute force to generate the PDFs and CDFs of the weighted mean revisit time metric for the baseline and threshold TROPICS constellations. The PDFs and CDFs of the 4-4-4, 6-6, 2-2-2, and 3-3 constellations are shown in Figure 20. They assume $P_f = 0.1$.

Looking at the CDFs, the robustness of the different constellations can be assessed as the probabilities of having a weighted mean revisit time of less than 60 minutes, which are 38.74%, 43.05%, 90.56% and 96.27% for the 2-2-2, 3-3, 6-6 and 4-4-4 configurations respectively. Therefore, we can observe the significant increase of coverage performance robustness of the 12-sat baseline architecture with respect to the 6-sat threshold architecture. For $P_f = 0.05$, The probabilities of having a weighted mean revisit time of less than 60 minutes are 63.02%, 66.34%, 97.23% and 99.2% for the 2-2-2, 3-3, 6-6 and 4-4-4 configurations respectively.

4.4. Constellation deployment and lifetime assessment

To complete the TROPICS constellation analysis, we apply a drag-based deployment strategy to calculate the time it takes to separate satellites in the same orbital plane efficiently.

In the deployment strategy considered, every TROPICS CubeSat, shown in Figure 22, has 3 different drag states, shown in Table 1, depending on the orientation of the solar arrays.

Low Drag	High Drag	Nominal Drag
100 cm^2	1300 cm^2	700 cm^2

Table 1: Drag states of the CubeSats

Having two satellites in the same orbital plane and starting off in the same exact position, the deployment strategy considered consists in setting one satellite to the low drag state and the other one to the high drag state during the eclipse part of the orbit, which for most LEO orbits – except for dawn-dusk orbits, which are not taken into consideration – is roughly 30%. Both satellites are set to the nominal drag state during the sunlight part of the orbit for power generating purposes. Due to the difference in drag areas, the satellites will slowly drift apart from each other during eclipses.

Figure 22: TROPICS space vehicle showing CubeSat bus, radiometer payload, and deployed articulated solar array

The simulation was run for 3 different hypothetical launch dates: January 2020, 2021 and 2022, to account for the effects of the solar cycle. Figure 21 shows that the results change significantly between these three scenarios. This is because, as shown in solar data prediction studies [57], solar activity starts increasing notably at the beginning of 2021 until 2025 and, therefore, the density of the atmosphere is affected significantly. In the worst case scenario (January 2020 launch date), at 600km and 30° inclination, the time it would take to separate 2 satellites 90 and 180 degrees in mean anomaly would be approximately 1.2 and 1.6 years respectively. On the other hand, in the best case scenario (January 2022 launch date) the time required to separate 2 satellites 90 and 180 degrees in mean anomaly

would be approximately 0.6 and 0.8 years, respectively. It is observed that the time to deployment (or time to operational orbit) is on the order of months and thus a significant portion of the spacecraft's lifetime.

Finally, we seek to assess if the lifetime of the TROPICS constellation exceeds NASA's 25 years de-orbiting recommendation[43]. As mentioned in Section 2.4, since lifetime depends mostly on the initial altitude of the constellation, this metric has been computed for different altitudes and considering both the nominal and high drag state configurations to account for useful –or operational– and de-orbiting lifetime, respectively. The results are presented in Table 2. The simulation start date was set to January 2005 due to the fact that predicted solar activity data was not available beyond 2030. There might exist some variability in the results when choosing a different simulation start date, and these changes would be more significant for those satellite's whose lifetime is less than the duration of a whole solar cycle, such as in 400km orbits.

Lifetime	400 km	500 km	600 km	700 km	800km
Operational	0.69	7.24	21.31	>25	>25
De-orbiting	0.32	4.50	14.89	>25	>25

Table 2: Satellite's useful and de-orbiting lifetimes in years for different satellite altitudes

These results suggest again that an altitude around 600km is the most suitable one for the TROPICS mission. Constellations with altitudes of 700km or 800km would need to incorporate de-orbiting strategies to fulfill NASA's 25-year deorbiting recommendation, as propulsion was deemed not a feasible option for the mission. On the other hand, choosing constellations below 500km would significantly reduce the mission's lifetime due to the increase in drag, which implies a faster satellite decay.

5. CONCLUSION

This paper described the process followed to define the constellation and orbit design for the NASA TROPICS mission. In doing so, the different figures of merit used to assess constellation coverage were discussed, and a new metric - continuous high rate revisit coverage - was introduced. Trade-offs between these metrics were discussed. A proxy metric for cost was also introduced that is based on energy considerations and thus independent of the pricing strategy of launch service provider.

For the TROPICS mission, we concluded that 30° inclination architectures provided better coverage metrics for the purpose of monitoring tropical storms. An altitude of 600km was chosen as a compromise between constellation deployment cost, coverage performance, spatial resolution, and lifetime. The threshold and baseline constellations (6 and 12 satellites, respectively) were suggested to meet certain mean and median revisit time requirements as well as a certain level of coverage robustness to hypothetical satellite and launch vehicle failures. We also observed that a higher number of planes implies shorter worst-case coverage gaps, thus achieving better higher percentiles statistics of mean revisit times, as well as mean response time and CHRC values.

Another finding for the TROPICS mission is that the Baseline constellation (e.g., 12 satellites distributed in 3 planes) is robust in coverage performance in the sense if one or more spacecraft fail, it is still capable of meeting TROPIC's mission requirements. We also noted that the higher percentiles of revisit times are the most sensitive metrics to hypothetical operational failures.

This paper also evaluated the viability of deploying evenly spaced satellites in the same plane using a strategy based on differential drag and without using propulsion, which consisted in changing the solar array configuration during eclipse/sunlight periods so that satellites in the same plane would drift apart from each other.

Finally, the useful lifetime and orbital decay of satellites was assessed for different altitudes to account for mission useful life and NASA's 25 year de-orbiting recommendation fulfillment. We concluded that orbits with higher altitudes than 600km would need to incorporate de-orbiting capabilities a part from drag to meet the 25 year recommendation. We also conclude that orbits below 500km would suffer from very fast satellite decay. Therefore, altitudes around 600km are the most suitable for this mission.

The methodology followed in this paper using design-by-shopping as a paradigm and focusing roughly on one variable at a time helped getting insight into how changes in decision variables affect the different FOMs considered. For instance, it was observed that the number of planes decision has a major impact on metrics such as mean response time, CHRC or cost, but not as much on other metrics such as mean revisit time. Other approaches could have been followed, such as multi-objective optimization over all variables- inclination, altitude, number of satellites and number of planes- at the same time. The result of that optimization process would have been a large Pareto front and, therefore, a strategy to choose a single architecture from that Pareto front should have been developed. One way to perform the best architecture selection is by defining weights for all the FOMs and do single objective optimization over all the architectures in the Pareto front. More generally, approaches based on value-driven design [58] define a value function (e.g., cost per image) that serves as the single objective to optimize, although in our experience such value functions are hard to define for Earth observation data products, with the potential exception of commercial optical or SAR imagery.

The proposed design-by-shopping framework for constellation design is generally applicable to Earth science missions other than the TROPICS mission. However, other missions may need to adapt the framework to their specific needs. For instance, the weights we used in the latitude-weighted metrics are only appropriate for applications focusing on tropical regions. Missions that require global vs partial coverage may choose to include/omit certain kinds of constellation geometries from the tradespace (high vs low inclinations and/or altitudes, Walker vs non-Walker/hybrid constellations). For example, while non-Walker constellations may show superior performance for missions with small or disjoint coverage regions.

Moreover, other FOMs may have to be considered instead of mean revisit time and/or mean response time (e.g., latency for a disaster monitoring mission). Finally, Earth observing systems with large vs small satellites may need different cost models and may choose different approaches to robustness. Generally speaking, the larger the satellite the more risk-averse decision-makers tend to be. That said, some of the insights revealed in this paper, such as guidelines about how to choose coverage and cost and robustness metrics for this process, remain of general interest to the community.

References

[1] W. Blackwell, S. Braun, R. Bennartz, C. Velden, M. DeMaria, R. Atlas, J. Dunion, F. Marks, R. Rogers, B. Annane, et al., An overview of the tropics nasa earth venture mission, Quarterly Journal of the Royal Meteorological Societydoi:10.1002/qj.3290.

[2] M. P. Ferringer, D. B. Spencer, Satellite constellation design tradeoffs using multiple-objective evolutionary computation, Journal of spacecraft and rockets 43 (6) (2006) 1404–1411. doi:https://doi.org/10.2514/1.18788.

[3] M. P. Ferringer, R. S. Clifton, T. G. Thompson, Constellation design with parallel multi-objective evolutionary computation, in: AIAA/AAS Astrodynamics Specialist Conference and Exhibit, 2006, p. 6015. doi:10.2514/6.2006-6015.

[4] M. P. Ferringer, R. S. Clifton, T. G. Thompson, Efficient and accurate evolutionary multi-objective optimization paradigms for satellite constellation design, Journal of Spacecraft and Rockets 44 (3) (2007) 682–691. doi:10.2514/1.26747.

[5] M. Ferringer, M. DiPrinzio, T. Thompson, K. Hanifen, P. Reed, A framework for the discovery of passive-control, minimum energy satellite constellations, in: AIAA/AAS Astrodynamics Specialist Conference, 2014, p. 4158. doi:10.2514/6.2014-4158.

[6] W. Mason, V. Coverstone-Carroll, J. Hartmann, Optimal earth orbiting satellite constellations via a pareto genetic algorithm, in: AIAA/AAS Astrodynamics Specialist Conference and Exhibit, 1998, p. 4381. doi:10.2514/6.1998-4381.

[7] I. Meziane-Tani, G. Métris, G. Lion, A. Deschamps, F. T. Bendimerad, M. Bekhti, Optimization of small satellite constellation design for continuous mutual regional coverage with multi-objective genetic algorithm, International Journal of Computational Intelligence Systems 9 (4) (2016) 627–637. doi:10.1080/18756891.2016.1204112.

[8] S. Nag, S. P. Hughes, J. Le Moigne, Streamlining the design tradespace for earth imaging constellations, in: AIAA SPACE 2016, 2016, p. 5561. doi:10.2514/6.2016-5561.

[9] W. R. Whittecar, M. P. Ferringer, Global coverage constellation design exploration using evolutionary algorithms, in: AIAA/AAS Astrodynamics Specialist Conference, 2014, p. 4159. doi:10.2514/6.2014-4159.

[10] E. A. Williams, W. A. Crossley, T. J. Lang, Average and maximum revisit time trade studies for satellite constellations using a multiobjective genetic algorithm, The Journal of the Astronautical Sciences 49 (3) (2001) 385–400.

[11] N. Hitomi, D. Selva, Constellation optimization using an evolutionary algorithm with a variable-length chromosome, in: IEEE Aerospace Conference, 2018. doi:10.1109/AERO.2018.8396743.

[12] M. P. Ferringer, D. B. Spencer, P. Reed, Many-objective reconfiguration of operational satellite constellations with the large-cluster epsilon non-dominated sorting genetic algorithm-ii, in: Evolutionary Computation, 2009. CEC'09. IEEE Congress on, IEEE, 2009, pp. 340–349. doi:10.1109/CEC.2009.4982967.

[13] J. Everist, T. N. Mundhenk, C. Landauer, K. Bellman, Visual surveillance coverage: strategies and metrics, in: Intelligent Robots and Computer Vision XXIII: Algorithms, Techniques, and Active Vision, Vol. 6006, International Society for Optics and Photonics, 2005, p. 600608.

[14] J. R. Wertz, D. F. Everett, J. J. Puschell, Space Mission Engineering: The New SMAD, Space Technology Library, Microcosm Press, 2011.

[15] P. Sengupta, S. R. Vadali, K. T. Alfriend, Satellite orbit design and maintenance for terrestrial coverage, Journal of Spacecraft and Rockets 47 (1) (2010) 177–187. doi:10.2514/1.44120.

[16] J. Zhang, F. Deng, X. He, L. Li, L. Zhang, Designing leo retrograde orbit satellite constellation for regional coverage, in: AIAA International Communications Satellite Systems Conference, Vol. 1, 2004, p. 3159. doi:10.2514/6.2004-3159.

[17] N. Crisp, K. Smith, P. Hollingsworth, Small satellite launch to leo: A review of current and future launch systems, Transactions of the Japan Society for Aeronautical and Space Sciences, Aerospace Technology Japan 12 (ists29) (2014) Tf_39–Tf_47. doi:10.2322/tastj.12.Tf_39.

[18] V. L. Foreman, J. Le Moigne, O. De Weck, A survey of cost estimating methodologies for distributed spacecraft missions, in: AIAA SPACE 2016, 2016, p. 5245. doi:10.2514/6.2016-5245.

[19] S. Nag, J. LeMoigne, O. de Weck, Cost and risk analysis of small satellite constellations for earth observation, in: Aerospace Conference, 2014 IEEE, IEEE, 2014, pp. 1–16. doi:10.1109/AERO.2014.6836396.

[20] N. H. Crisp, K. Smith, P. Hollingsworth, Launch and deployment of distributed small satellite systems, Acta Astronautica 114 (2015) 65–78. doi:10.1016/j.actaastro.2015.04.015.

[21] W. Hohmann, Die erreichbarkeit der himmelskörper. untersuchungen über das raumfahrtproblem., Die Erreichbarkeit der Himmelskörper. Untersuchungen über das Raumfahrtproblem., by Hohmann, W.. Oldenbourg, München (Germany), 1994, 122 p., ISBN 3-486-23106-5, Price DM 29.80.

[22] J. Depasquale, A. Charania, H. Kanamaya, S. Matsuda, Analysis of the earth-to-orbit launch market for nano and microsatellites, in: AIAA SPACE 2010 Conference & Exposition, 2010, p. 8602. doi:10.2514/6.2010-8602.

[23] R. Lab, Rocket lab launch services.
URL `https://www.rocketlabusa.com/launch/`

[24] A. Rossi, G. B. Valsecchi, P. Farinella, Risk of collisions for constellation satellites, Nature 399 (6738) (1999) 743. doi:10.1038/21565.

[25] I.-S. Chang, Space launch vehicle reliability, Crosslink (2005) 22–32.

[26] R. D. Luders, Satellite networks for continuous zonal coverage, ARS Journal 31 (2) (1961) 179–184. doi:doi.org/10.2514/8.5422.

[27] J. G. Walker, Continuous whole-earth coverage by circular-orbit satellite patterns, Tech. rep., ROYAL AIRCRAFT ESTABLISHMENT FARNBOROUGH (UNITED KINGDOM) (1977).

[28] A. H. Ballard, Rosette constellations of earth satellites, IEEE Transactions on Aerospace and Electronic Systems AES-16 (5) (1980) 656–673. doi:10.1109/TAES.1980.308932.

[29] L. Rider, Optimized polar orbit constellations for redundant earth coverage, Journal of the Astronautical Sciences 33 (1985) 147–161.

[30] J. E. Draim, Three-and four-satellite continuous-coverage constellations, Journal of Guidance, Control, and Dynamics 8 (6) (1985) 725–730. doi:10.2514/3.20047.

[31] T. J. Lang, Symmetric circular orbit satellite constellations for continuous global coverage, in: Astrodynamics 1987, 1988, pp. 1111–1132.

[32] J. E. Draim, Continuous global n-tuple coverage with (2n+ 2) satellites, Journal of Guidance, Control, and Dynamics 14 (1) (1991) 17–23. doi:10.2514/3.20599.

[33] L. Rider, Analytic design of satellite constellations for zonal earth coverage using inclined circular orbits, Journal of the Astronautical Sciences 34 (1986) 31–64.

[34] W. S. Adams, L. Rider, Circular polar constellations providing continuous single or multiple coverage above a specified latitude, Journal of the Astronautical Sciences 35 (1987) 155–192.

[35] T. J. Lang, Low earth orbit satellite constellations for continuous coverage of the mid-latitudes, in: Astrodynamics Conference, 2013, p. 3638. doi:10.2514/6.1996-3638.

[36] T. Ely, R. Anderson, Y. Bar-Sever, D. Bell, J. Guinn, M. Jah, P. Kallemeyn, E. Levene, L. Romans, S. Wu, Mars network constellation design drivers and strategies, in: AAS/AIAA Astrodynamics Specialist Conference, 1999, p. 301.

[37] E. Lansard, E. Frayssinhes, J.-L. Palmade, Global design of satellite constellations: a multi-criteria performance comparison of classical walker patterns and new design patterns, Acta Astronautica 42 (9) (1998) 555–564. doi:10.1016/S0094-5765(98)00043-5.

[38] J. Grosshans, M. F. Barschke, Mission concept of a nanosatellite constellation for global wildfire monitoring, in: AIAA SPACE and Astronautics Forum and Exposition, 2017, p. 5267. doi:10.2514/6.2017-5267.

[39] G. F. Dubos, J. H. Saleh, Comparative cost and utility analysis of monolith and fractionated spacecraft using failure and replacement markov models, Acta Astronautica 68 (1-2) (2011) 172–184. doi:10.1016/j.actaastro.2010.07.011.

[40] J.-F. Castet, J. H. Saleh, Interdependent multi-layer networks: Modeling and survivability analysis with applications to space-based networks, PloS one 8 (4) (2013) e60402. doi:10.1371/journal.pone.0060402.

[41] J.-F. Castet, J. H. Saleh, Satellite reliability: statistical data analysis and modeling, Journal of Spacecraft and Rockets 46 (5) (2009) 1065–1076. doi:10.2514/1.42243.

[42] A. L. Weigel, D. E. Hastings, Evaluating the cost and risk impacts of launch choices, Journal of Spacecraft and Rockets 41 (1) (2004) 103–110. doi:10.2514/1.9270.

[43] S. M. Hull, End of mission considerations, Preprint GSFC.BOOK.7496.2012, NASA Goddard Space Flight Center, Greenbelt, MD, United States (01 2013).

[44] J. Puig-Suari, G. Zohar, K. Leveque, Deployment of cubesat constellations utilizing current launch opportunities, in: AIAA/USU Small Satellite Conference, no. 15, 2013.

[45] M. Fakoor, M. Bakhtiari, M. Soleymani, Optimal design of the satellite constellation arrangement reconfiguration process, Advances in Space Research 58 (3) (2016) 372–386. doi:10.1016/j.asr.2016.04.031.

[46] C. L. Leonard, W. M. Hollister, E. V. Bergmann, Orbital formationkeeping with differential drag, Journal of Guidance, Control, and Dynamics 12 (1) (1989) 108–113. doi:10.2514/3.20374.

[47] R. Bevilacqua, M. Romano, Rendezvous maneuvers of multiple spacecraft using differential drag under j2 perturbation, Journal of Guidance, Control, and Dynamics 31 (6) (2008) 1595–1607. doi:10.2514/1.36362.

[48] B. S. Kumar, A. Ng, K. Yoshihara, A. De Ruiter, Differential drag as a means of spacecraft formation control, in: Aerospace Conference, 2007 IEEE, 2007, pp. 1–9. doi:10.1109/AERO.2007.352790.

[49] S. Varma, K. D. Kumar, Multiple satellite formation flying using differential aerodynamic drag, Journal of Spacecraft and Rockets 49 (2) (2012) 325–336. doi:10.2514/1.52395.

[50] M. Horsley, S. Nikolaev, A. Pertica, Small satellite rendezvous using differential lift and drag, Journal of Guidance, Control, and Dynamics 36 (2) (2013) 445–453. doi:10.2514/1.57327.

[51] O. Ben-Yaacov, P. Gurfil, Long-term cluster flight of multiple satellites using differential drag, Journal of Guidance, Control, and Dynamics 36 (6) (2013) 1731–1740. doi:10.2514/1.61496.

[52] T. Finley, D. Rose, K. Nave, W. Wells, J. Redfern, R. Rose, C. Ruf, Techniques for leo constellation deployment and phasing utilizing differential aerodynamic drag, Advances in the Astronautical Sciences 150 (2014) 1397–1411.

[53] S. Lab, Orbit propagation simulator: Orekit with seaklab specific functionality, `https://github.com/seakers/orekit/tree/dev` (2018).

[54] S. Bruinsma, G. Thuillier, F. Barlier, The dtm-2000 empirical thermosphere model with new data assimilation and constraints at lower boundary: accuracy and properties, Journal of Atmospheric and Solar-Terrestrial Physics 65 (9) (2003) 1053–1070. doi:10.1016/S1364-6826(03)00137-8.

[55] W. Blackwell, G. Allen, C. Galbraith, R. Leslie, I. Osaretin, M. Scarito, M. Shields, E. Thompson, D. Toher, D. Townzen, et al., Micromas: A first step towards a nanosatellite constellation for global storm observation, in: AIAA/USU Small Satellite Conference, no. 1, 2013.

[56] W. M. Organization, Observing systems capability analysis and review tool observation requirements.
URL `https://www.wmo-sat.info/oscar/requirements`

[57] W. D. Pesnell, K. H. Schatten, An early prediction of the amplitude of solar cycle 25, Solar Physics 293 (7) (2018) 112. doi:10.1007/s11207-018-1330-5.

[58] P. D. Collopy, P. M. Hollingsworth, Value-driven design, Journal of aircraft 48 (3) (2011) 749–759. doi:10.2514/1.C000311.